Supporting Information for Chiral carbon nanorings with strong chiral luminescent and second harmonic generation properties

Qi Yu,[ab†] Jinghan Zhao,[ad†] Zuo Xiao,[*ab] Yu Wang,[a] Ke Jin,[c] Kaige Huang,[e] Chuantian Zuo,[ab] Lingyun Zhu,[*ab] Wenna Du,[*ab] Shizhong Yue,[e] Zhijie Wang,[*e] Xinfeng Liu,[ab] and Liming Ding[*c]

[a]National Center for Nanoscience and Technology, Beijing 100190, China. E-mail: xiaoz@nanoctr.cn; zhuly@nanoctr.cn; duwn@nanoctr.cn
[b]University of Chinese Academy of Sciences, Beijing 100049, China.
[c]School of Chemical Engineering and Light Industry, Guangdong University of Technology, Guangzhou 510006, China. E-mail: ding@gdut.edu.cn
[d]Advanced Research Institute of Multidisciplinary Sciences, Beijing Institute of Technology, Beijing 100081, China.
[e]Institute of Semiconductors, Chinese Academy of Sciences, Beijing 100083, China. E-mail: wangzj@semi.ac.cn
† These authors contributed equally to this work.

1. General characterization

^{1}H and ^{13}C NMR spectra were measured on a Bruker Avance-400 spectrometer. 2D NMR spectra were measured on a Bruker Avance-600 spectrometer. IR spectra were measured on a PerkinElmer SP-200i spectrophotometer. Absorption spectra were recorded on a Shimadzu UV-1800 spectrophotometer. Single-crystal X-ray diffraction data of compound D_3-(*P*)-NR5 and D_3-(*M*)-NR5 were collected on a Bruker D8 Venture diffractometer equipped with Ga Kα radiation (λ = 1.34139) at 170.0 K. Structures were solved by intrinsic phasing method using SHELXT[1] and refined by full matrix least-squares on F^2 using SHELXL-2018[2] within the OLEX2 GUI[3]. All non-hydrogen atoms were refined anisotropically. All hydrogen atoms were positioned geometrically and refined as riding. Circular dichroism (CD) spectra were recorded on a JASCO J-1500 spectrophotometer. Circularly polarized luminescence (CPL) spectra were measured by using a JASCO CPL-200 spectrophotometer. The absolute quantum yields and emission spectra were measured on a HORIBA FluoroMax Plus spectrophotometer. The light source used for SHG characterization is a picosecond laser with a central wavelength of 1064 nm, featuring a pulse duration of 15 ps, a repetition rate of 80 MHz, and an average power of 1 mW. The laser beam is focused onto the sample through a 100× objective lens (NA = 0.9). The generated SHG signal is collected by the same lens, filtered through a short-pass filter and detected by a spectrometer. For polarization-dependent SHG measurements, we controlled the laser polarization by rotating the half-wave plate in front of the objective lens. For SHG-CD measurements, the half-wave plate was replaced by a quarter-wave plate to modulate excitation polarization between LCP and RCP states.

2. Computational details

The molecular geometries of the ground state were optimized by density functional theory (DFT) at the B3LYP/6-31G(d,p) level The excited-state properties were calculated by time-dependent DFT (TDDFT) theory at the B3LYP/6-31G(d,p) level. The simulated CD spectra are obtained by Gaussian convolution in the following form:

$$\mathrm{CD}(E) = \frac{1}{2.297 \times 10^{-39}\sqrt{2\pi\sigma}} \frac{1}{\sum_i} \Delta E_{0i} R_{0i} \exp\left(-\left[\frac{E-\Delta E_{0i}}{2\sigma}\right]^2\right)$$

σ is a broadening factor, which is set to be 0.1 eV. ΔE_{0i} and R_{0i} represent the excitation energy and the rotational strength, respectively, for the transition from the ground state $|0\rangle$ to the excited state $|i\rangle$. All the calculations were carried out using Gaussian16 software.[4]

3. Synthesis

All reagents were purchased from J&K Co., Aladdin Co., Innochem Co., and other commercial suppliers. All reactions dealing with air- or moisture-sensitive compounds were carried out by using standard Schlenk techniques.

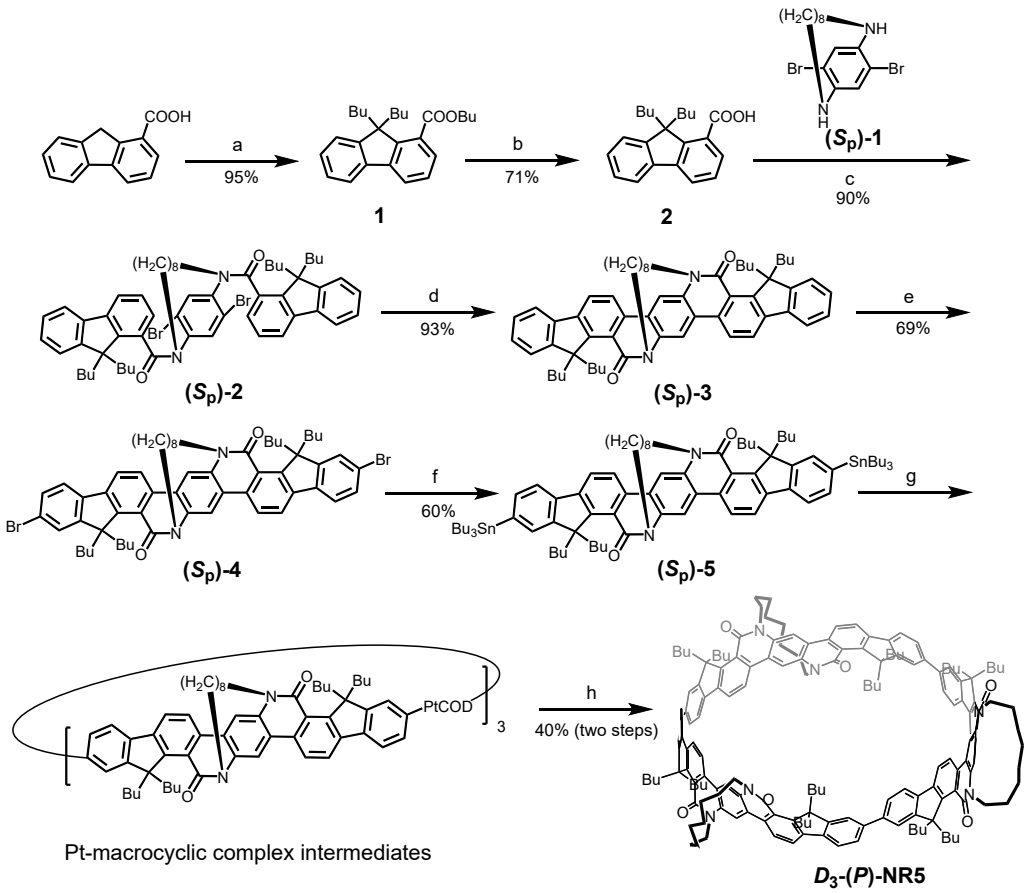

Scheme S1. The synthetic route for D_3-(*P*)-NR5. Reaction conditions: a) C_4H_9Br/KOH; b) H_2O/KOH; c) 1. $C_2O_2Cl_2$, 2. NEt_3; d) $Pd(OAc)_2/PCy_3 \cdot HBF_4/Cs_2CO_3$; e) NBS/TFA; f) $Pd(OAc)_2/PCy_3/(Bu_3Sn)_2$; g) $(COD)PtCl_2$; h) PPh_3, Tol, 110 °C

Compound 1. 9H-Fluorene-1-carboxylic acid (1 g, 4.76 mmol) and tetrabutylammonium bromide (306 mg, 0.95 mmol) were added to Schlenk tube, and the tube was purged with nitrogen three times. 1-Bromobutane (10.3 mL, 95.5 mmol) and 5.3 mL of potassium hydroxide aqueous solution (1 g/mL) were added under nitrogen. The reaction mixture was stirred at 60 °C for 12 h. The reaction mixture was washed with water and extracted with CH_2Cl_2 for three times. After removal of the solvent under reduced pressure, the crude product was purified via column chromatography (silica gel) by using petroleum ether:CH_2Cl_2 (4:1) as eluent to give compound **1** as a colorless oily liquid (1.8 g, 95%). ^{1}H NMR ($CDCl_3$, 400 MHz, δ/ppm): 7.86 (d, *J* = 7.6 Hz, 1H), 7.73-7.69 (m, 2H), 7.40 (t, *J* = 7.6 Hz, 1H), 7.36-7.33 (m, 3H), 4.37 (t, *J* = 6.7 Hz, 2H), 2.61 (td, *J* = 12.7, 4.8 Hz, 2H), 1.94 (td, *J* = 12.6, 4.5 Hz, 2H), 1.83-1.76 (m, 2H), 1.50 (h, *J* = 7.4 Hz, 2H), 1.06-0.98 (m, 7H), 0.63 (t, *J* = 7.4 Hz, 6H), 0.53-0.42 (m, 4H). ^{13}C NMR ($CDCl_3$, 100 MHz, δ/ppm): 167.92, 151.82, 149.08, 143.10, 139.72, 129.49, 128.60, 127.75, 126.79, 126.62, 122.74, 122.31, 119.12, 64.93, 57.61, 38.50, 30.80, 26.00, 22.91, 19.29, 13.74.

Compound 2. To a solution of compound 1 (1.8 g, 4.76 mmol) in THF (24 mL)/EtOH (24 mL)/H_2O (6 mL) was added potassium hydroxide (1.33 g, 23.75 mmol). The reaction mixture was stirred at 70 °C for 12 h. Then, the reaction mixture was cooled to room temperature and was acidified by diluted hydrochloric acid. The mixture was extracted with CH_2Cl_2 for three times. After removal of CH_2Cl_2 under reduced pressure, the crude product was purified via column chromatography (silica gel) by using ethyl acetate:CH_2Cl_2 (3:100) as eluent to give compound **2** as a white solid (1.15 g, 71%). ^{1}H NMR ($CDCl_3$, 400 MHz, δ/ppm): 11.71 (br, 1H), 7.99 (dd, *J* = 24.4, 7.6 Hz, 2H), 7.73-7.71 (m, 1H), 7.47 (t, *J* = 7.7 Hz, 1H), 7.39-7.36 (m, 3H), 2.78 (td, *J* = 12.7, 4.8 Hz, 2H), 1.97 (td, *J* = 12.6, 4.6 Hz, 2H), 1.10-1.02 (m, 4H), 0.65 (t, *J* = 7.3 Hz, 6H), 0.53-0.38 (m, 4H). ^{13}C NMR ($CDCl_3$, 100 MHz, δ/ppm): 172.99, 151.99, 150.70, 143.60, 139.44, 129.94, 127.96, 127.59, 127.02, 126.70, 124.16, 122.36, 119.12, 58.07, 38.17, 26.08, 22.90, 13.71.

Compound (S_p)-2. To a solution of compound 2 (956 mg, 2.97 mmol) in dry CH_2Cl_2 (20 mL) was added oxalyl chloride solution (4.55 mL, 2M in CH_2Cl_2, 9.1 mmol) under nitrogen. A drop of dry DMF was added as the catalyst. The reaction mixture was stirred at room temperature for 2 h. After removal of the solvent under reduced pressure, the acyl chloride intermediate was obtained as a yellow solid and was directly subjected to the next step reaction. To the solution of the acyl chloride intermediate in dry THF (20 mL) was added triethylamine (2 mL, 14.46 mmol) and (S_p)-1 (446 mg, 1.19 mmol) under argon. After stirring at 70 °C for 12 h, the reaction was quenched with water and extracted with CH_2Cl_2 for three times. The combined organic layer was concentrated under reduced pressure. The crude product was purified via column chromatography (silica gel) by using CH_2Cl_2 as eluent to give compound **(S_p)-2** as a white solid (1.05 g, 90%). Due to the presence of rotational isomers, the NMR spectra exhibit broadening and multiple peaks. ^{1}H NMR ($CDCl_3$, 400 MHz, δ/ppm): 7.82-6.78 (br, aromatic protons,16H), 4.61-0.25 (br, aliphatic protons, 52H). ^{13}C NMR ($CDCl_3$, 100 MHz, δ/ppm): 169.58, 151.05, 146.74, 143.02, 140.37, 139.94, 136.98, 132.20, 127.80, 126.97, 126.74, 125.23, 122.82, 122.46, 121.60, 120.62, 119.44, 57.32, 57.02, 51.11, 41.92, 41.09, 39.26, 37.81, 26.65, 26.33,

25.85, 23.58, 23.39, 22.94, 13.94.

Compound (S_p)-3. To a solution of compound (S_p)-2 (900 mg, 0.92 mmol) in dry DMA (18 mL) was added palladium diacetate (82 mg, 0.37 mmol), tricyclohexylphosphonium tetrafluoroborate (202 mg, 0.55 mmol) and cesium carbonate (1.19 g, 3.66 mmol) under nitrogen. The reaction mixture was stirred at 130 °C for 5 min. The color of the reaction mixture turned black. The reaction mixture was washed with water and extracted with CH_2Cl_2 for three times. After removal of the solvent under reduced pressure, the crude product was purified via column chromatography (silica gel) by using petroleum ether:CH_2Cl_2 (1:2) as eluent to give **(S_p)-3** as a yellow solid (700 mg, 93%). ^{1}H NMR ($CDCl_3$, 400 MHz, δ/ppm): 8.18-8.11 (m, 3H), 7.77-7.74 (m, 1H), 7.46-7.44 (m, 1H), 7.41-7.35 (m, 2H), 5.20-5.14 (m, 1H), 4.24-4.17 (m, 1H), 3.52 (td, J = 12.4, 4.9 Hz, 1H), 3.08 (td, J = 13.2, 5.2 Hz, 1H), 2.06-1.97 (m, 2H), 1.79 (s, 1H), 1.61 (s, 1H), 1.09-0.95 (m, 5H), 0.84 (s, 1H), 0.62 (td, J = 7.3, 4.7 Hz, 7H), 0.56-0.39 (m, 4H), 0.05 (s, 1H). ^{13}C NMR ($CDCl_3$, 100 MHz, δ/ppm): 161.23, 153.78, 151.87, 144.22, 139.19, 134.11, 132.62, 128.11, 126.54, 125.07, 123.62, 122.99, 122.59, 122.32, 118.84, 111.04, 59.86, 45.08, 38.73, 35.98, 28.84, 26.67, 26.28, 26.23, 23.02, 22.82, 13.83, 13.80.

Compound (S_p)-4. To a solution of compound (S_p)-3 (600 mg, 0.73 mmol) in $CHCl_3$ (30 mL)/trifluoroacetic acid (12 mL) was added N-bromosuccinimide (325 mg, 1.83 mmol). After stirring at room temperature for 12 h in the dark, the reaction mixture was neutralised with aqueous sodium bicarbonate and extracted with CH_2Cl_2 for three times. After removal of the solvent, the crude product was purified via column chromatography (silica gel) by using petroleum ether:CH_2Cl_2 (3:1) as eluent to give **(S_p)-4** as a yellow solid (494 mg, 69%).^{1}H NMR ($CDCl_3$, 400 MHz, δ/ppm): 8.18-8.06 (m, 3H), 7.62-7.58 (m, 2H), 7.49 (dd, J = 8.0, 1.7 Hz, 1H), 5.16 (ddd, J = 14.3, 6.0, 3.9 Hz, 1H), 4.23-4.17 (m, 1H), 3.57-3.49 (m, 1H), 3.12-3.04 (m, 1H), 2.0-1.90 (m, 2H), 1.78 (s, 1H), 1.60 (s, 1H), 1.08-1.03 (m, 4H), 0.94 (s, 1H), 0.83 (s, 1H), 0.65-0.61 (m, 7H), 0.53-0.41 (m, 4H), 0.02 (s, 1H). ^{13}C NMR ($CDCl_3$, 100 MHz, δ/ppm): 161.04, 155.99, 151.55, 143.13, 138.17, 134.16, 132.93, 129.83, 125.91, 125.06, 123.66, 122.96, 122.57, 122.26, 120.26, 111.13, 60.20, 45.12, 38.63, 35.91, 28.82, 26.67, 26.62, 26.27, 26.23, 22.96, 22.75, 13.82, 13.79.

Compound (S_p)-5. To a solution of compound (S_p)-4 (400 mg, 0.41 mmol) in toluene (40 mL) was added palladium diacetate (11 mg, 0.05 mmol), tricyclohexyl phosphine (27.5 mg, 0.10 mmol) and hexabutylditin (0.83 mL, 1.64 mmol) under nitrogen. The reaction mixture was stirred at 110 °C for 12 h. The reaction mixture was purified via column chromatography (silica gel) by using petroleum ether:NEt_3 (3:1) as eluent to give compound **(S_p)-5** as a yellow solid (344 mg, 60%). Due to the instability of (S_p)-5, it was directly subjected to the next-step reaction without further characterization.

Compound D_3-(P)-NR5. To a solution of compound (S_p)-5 (243 mg, 0.17 mmol) in dry 1,2-dichloroethane (20 mL) was added 1,5-cyclooctadieneplatinum (II) dichloride (64.8 mg, 0.17 mmol) under nitrogen. After stirring at 70°C for 24 h, solvent was removed under reduced

pressure and the crude product of Pt-macrocyclic complex intermediates was dried under vacuum at room temperature for 1 h. To a solution of the Pt-macrocyclic intermediates in toluene (50 mL) was added triphenylphosphine (1.5 g, 5.73 mmol) under nitrogen. The reaction mixture was stirred for 10 min at room temperature and then refluxed at 110°C for 2h. After removal of the solvent, the crude product was purified via column chromatography (silica gel) by using $CHCl_3$:ethyl acetate (100:1) as eluent to give ***D*$_3$-(*P*)-NR5** as a yellow solid (57 mg, 40%). ^{1}H NMR ($CDCl_3$, 400 MHz, δ/ppm): 7.91 (dd, *J* = 17.8, 8.3 Hz, 4H), 7.63 (d, *J* = 8.2 Hz, 1H), 7.57 (d, *J* = 7.9 Hz, 1H), 5.07-5.04 (m, 1H), 4.08-4.03 (m, 1H), 3.04 (td, *J* = 12.2, 4.5 Hz, 1H), 2.81 (td, *J* = 16, 4 Hz, 1H), 2.26 (td, *J* = 12.3, 4.3 Hz, 1H), 2.08 (td, *J* = 13.0, 4.5 Hz, 1H), 1.83-1.73 (m, 2H), 1.26-1.12 (m, 3H), 1.07-1.02 (m,1H), 0.98-0.93 (m, 3H), 0.75 (t, *J* = 7.2 Hz, 6H), 0.54 (t, *J* = 7.4 Hz, 3H), 0.11-0.02 (m, 2H). ^{13}C NMR ($CDCl_3$, 100 MHz, δ/ppm): 161.85, 154.11, 152.11, 143.51, 139.07, 138.66, 134.97, 131.20, 126.16, 125.74, 123.63, 123.50, 121.47, 119.99, 119.18, 110.96, 59.58, 45.01, 40.78, 34.25, 29.29, 27.16, 26.84, 26.07, 25.90, 23.13, 22.61, 14.07, 13.39. MALDI-TOF HRMS (m/z): $C_{174}H_{192}N_6O_6$ [M^+] calc. 2461.4903, found 2461.4887.

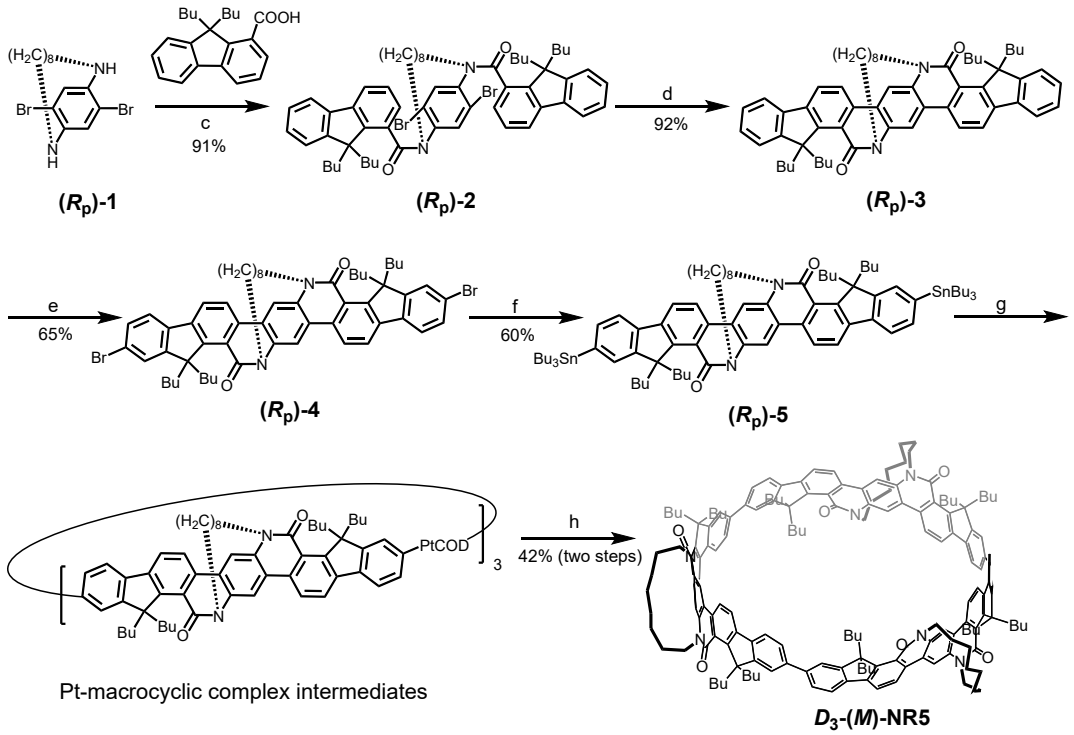

Scheme S2. The synthetic route for *D*$_3$-(*M*)-NR5. Reaction conditions: c) 1. $C_2O_2Cl_2$, 2. NEt_3; d) $Pd(OAc)_2/PCy_3{\cdot}HBF_4/Cs_2CO_3$; e) NBS/TFA; f) $Pd(OAc)_2/PCy_3/(Bu_3Sn)_2$; g) $(COD)PtCl_2$; h) PPh_3, Tol, 110 °C

Compound (*R*$_p$)-2. To a solution of compound 2 (940 mg, 2.92 mmol) in dry CH_2Cl_2 (20 mL) was added oxalyl chloride solution (4.38 mL, 2M in CH_2Cl_2, 8.76 mmol) under nitrogen. A drop of dry DMF was added as the catalyst. The reaction mixture was stirred at room temperature for 2 h. After removal of the solvent under reduced pressure, the acyl chloride intermediate was obtained as a yellow solid and was directly subjected to the next step reaction.

To the solution of the acyl chloride intermediate in dry THF (20 mL) was added triethylamine (2 mL, 14.46 mmol) and (R_p)-1 (439 mg, 1.17 mmol) under argon. After stirring at 70 °C for 12 h, the reaction was quenched with water and extracted with CH_2Cl_2 for three times. The combined organic layer was concentrated under reduced pressure. The crude product was purified via column chromatography (silica gel) by using CH_2Cl_2 as eluent to give **(R_p)-2** as a white solid (1.04 g, 91%). Due to the presence of rotational isomers, the NMR spectra exhibit broadening and multiple peaks. ^{1}H NMR ($CDCl_3$, 400 MHz, δ/ppm): 7.82-6.80 (br, aromatic protons,16H), 4.61-0.25 (br, aliphatic protons, 52H). ^{13}C NMR ($CDCl_3$, 100 MHz, δ/ppm): 169.60, 151.06, 146.74, 143.03, 140.37, 139.94, 136.98, 132.24, 127.80, 126.99, 126.74, 125.23, 122.83, 122.47, 121.61, 120.62, 119.44, 57.32, 57.02, 51.07, 41.92, 41.05, 39.28, 37.81, 26.66, 26.33, 25.86, 23.59, 23.39, 22.94, 13.93.

Compound (R_p)-3. To a solution of compound (R_p)-2 (900 mg, 0.92 mmol) in dry DMA (18 mL) was added palladium diacetate (82 mg, 0.37 mmol), tricyclohexylphosphonium tetrafluoroborate (202 mg, 0.55 mmol) and cesium carbonate (1.19 g, 3.66 mmol) under nitrogen. The reaction mixture was stirred at 130 °C for 5 min. The color of the reaction mixture turned black. The reaction mixture was washed with water and extracted with CH_2Cl_2 for three times. After removal of the solvent under reduced pressure, the crude product was purified via column chromatography (silica gel) by using petroleum ether:CH_2Cl_2 (1:2) as eluent to give **(R_p)-3** as a yellow solid (695 mg, 92%). ^{1}H NMR ($CDCl_3$, 400 MHz, δ/ppm): 8.18-8.11 (m, 3H), 7.77-7.74 (m, 1H), 7.47-7.44 (m, 1H), 7.42-7.35 (m, 2H), 5.20-5.14 (m, 1H), 4.24-4.17 (m, 1H), 3.52 (td, J = 12.4, 4.9 Hz, 1H), 3.08 (td, J = 13.2, 5.2 Hz, 1H), 2.06-1.97 (m, 2H), 1.79 (s, 1H), 1.60 (s, 1H), 1.09-0.93 (m, 5H), 0.84 (s, 1H), 0.62 (td, J = 7.4, 4.6 Hz, 7H), 0.54-0.4 (m, 4H), 0.04 (s, 1H). ^{13}C NMR ($CDCl_3$, 100 MHz, δ/ppm): 161.22, 153.78, 151.87, 144.22, 139.18, 134.10, 132.61, 128.11, 126.53, 125.06, 123.62, 122.99, 122.59, 122.32, 118.83, 111.04, 59.86, 45.08, 38.73, 35.98, 28.83, 26.67, 26.28, 26.22, 23.01, 22.82, 13.82, 13.79.

Compound (R_p)-4. To a solution of compound (R_p)-3 (600 mg, 0.73 mmol) in $CHCl_3$ (30 mL)/trifluoroacetic acid (12 mL) was added N-bromosuccinimide (325 mg, 1.83 mmol). After stirring at room temperature for 12 h in the dark, the reaction mixture was neutralised with aqueous sodium bicarbonate and extracted with CH_2Cl_2 for three times. After removal of the solvent, the crude product was purified via column chromatography (silica gel) by using petroleum ether:CH_2Cl_2 (3:1) as eluent to give **(R_p)-4** as a yellow solid (465 mg, 65%). ^{1}H NMR ($CDCl_3$, 400 MHz, δ/ppm): 8.18-8.06 (m, 3H), 7.62-7.58 (m, 2H), 7.49 (dd, J = 8.0, 1.7 Hz, 1H), 5.16 (dt, J = 14.8, 4.8 Hz, 1H), 4.22-4.17 (m, 1H), 3.54 (td, J = 12.5, 11.9, 5.7 Hz, 1H), 3.13-3.05 (m, 1H), 2.03-1.91 (m, 2H), 1.78 (s, 1H), 1.59 (s, 1H), 1.08-1.03 (m, 4H), 0.94 (s, 1H), 0.83 (s, 1H), 0.65-0.60 (m, 7H), 0.53-0.42 (m, 4H), 0.02 (s, 1H). ^{13}C NMR ($CDCl_3$, 100 MHz, δ/ppm): 161.05, 155.99, 151.55, 143.14, 138.18, 134.17, 132.94, 129.84, 125.92, 125.07, 123.66, 122.96, 122.57, 122.26, 120.26, 111.14, 60.20, 45.12, 38.63, 35.92, 28.82, 26.67, 26.63, 26.28, 26.23, 22.96, 22.75, 13.82, 13.79.

Compound (R_p)-5. To a solution of compound (R_p)-4 (400 mg, 0.41 mmol) in toluene (40 mL) was added palladium diacetate (11 mg, 0.05 mmol), tricyclohexyl phosphine (28 mg, 0.10

mmol) and hexabutylditin (0.83 mL, 1.64 mmol) under nitrogen. The reaction mixture was stirred at 110 °C for 12 h. The reaction mixture was purified via column chromatography (silica gel) by using petroleum ether:NEt_3 (3:1) as eluent to give compound **(R_p)-5** as a yellow solid (344 mg, 60%). Due to the instability of (R_p)-5, it was directly subjected to the next-step reaction without further characterization.

Compound *D*$_3$-(*M*)-NR5. To a solution of compound (R_p)-5 (300 mg, 0.21 mmol) in dry 1,2-dichloroethane (20 mL) was added 1,5-cyclooctadieneplatinum (II) dichloride (79 mg, 0.21 mmol) under nitrogen. After stirring at 70°C for 24 h, solvent was removed under reduced pressure and the crude product of Pt-macrocyclic complex intermediates was dried under vacuum at room temperature for 1 h. To a solution of the Pt-macrocyclic intermediates in toluene (50 mL) was added triphenylphosphine (1.65 g, 6.3 mmol) under nitrogen. The reaction mixture was stirred for 10 min at room temperature and then refluxed at 110°C for 2h. After removal of the solvent, the crude product was purified via column chromatography (silica gel) by using $CHCl_3$:ethyl acetate (100:1) as eluent to give ***D*$_3$-(*M*)-NR5** as a yellow solid (72 mg, 42%). ^{1}H NMR ($CDCl_3$, 400 MHz, δ/ppm): 7.91 (dd, *J* = 17.6, 8.2 Hz, 4H), 7.63 (d, *J* = 8.1 Hz, 1H), 7.57 (d, *J* = 8.2 Hz, 1H), 5.07-5.04 (m, 1H), 4.08-4.03 (m, 1H), 3.04 (td, *J* = 11.9, 4.2 Hz, 1H), 2.81 (td, *J* = 12.8, 5.1 Hz, 1H), 2.26 (td, *J* = 12.3, 4.3 Hz, 1H), 2.08 (td, *J* = 13.0, 4.5 Hz, 1H), 1.84-1.73 (m, 2H), 1.26-1.12 (m, 3H), 1.07-1.02 (m,1H), 0.95 (dd, *J* = 13.7, 6.6 Hz, 3H), 0.75 (t, *J* = 7.2 Hz, 6H), 0.54 (t, *J* = 7.3 Hz, 3H), 0.11-0.02 (m, 2H). ^{13}C NMR ($CDCl_3$, 100 MHz, δ/ppm): 161.85, 154.11, 152.11, 143.51, 139.07, 138.66, 134.97, 131.20, 126.16, 125.74, 123.63, 123.50, 121.47, 119.99, 119.18, 110.96, 59.58, 45.01, 40.78, 34.25, 29.29, 27.16, 26.84, 26.07, 25.90, 23.13, 22.61, 14.07, 13.39. MALDI-TOF HRMS (m/z): $C_{174}H_{192}N_6O_6$ [M^+] calc. 2461.4903, found 2461.4889.

4. ^{1}H, ^{13}C and 2D NMR spectra

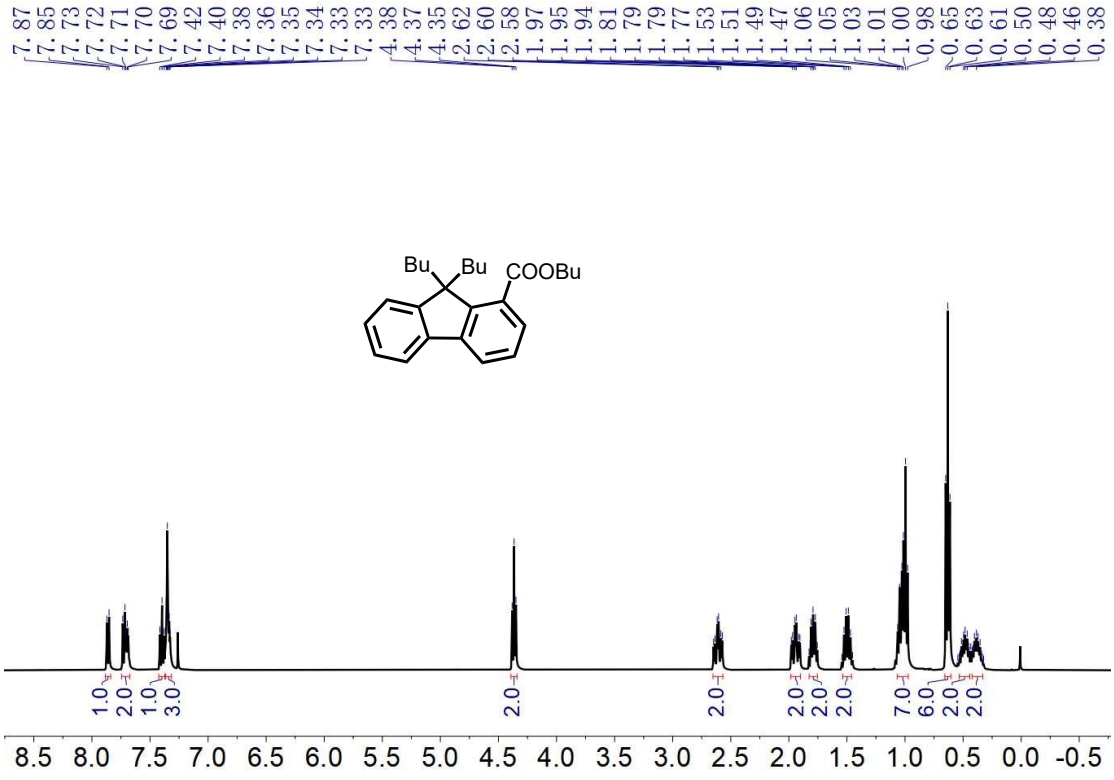

Figure S1. ^{1}H NMR spectrum for compound **1** ($CDCl_3$, 298K)

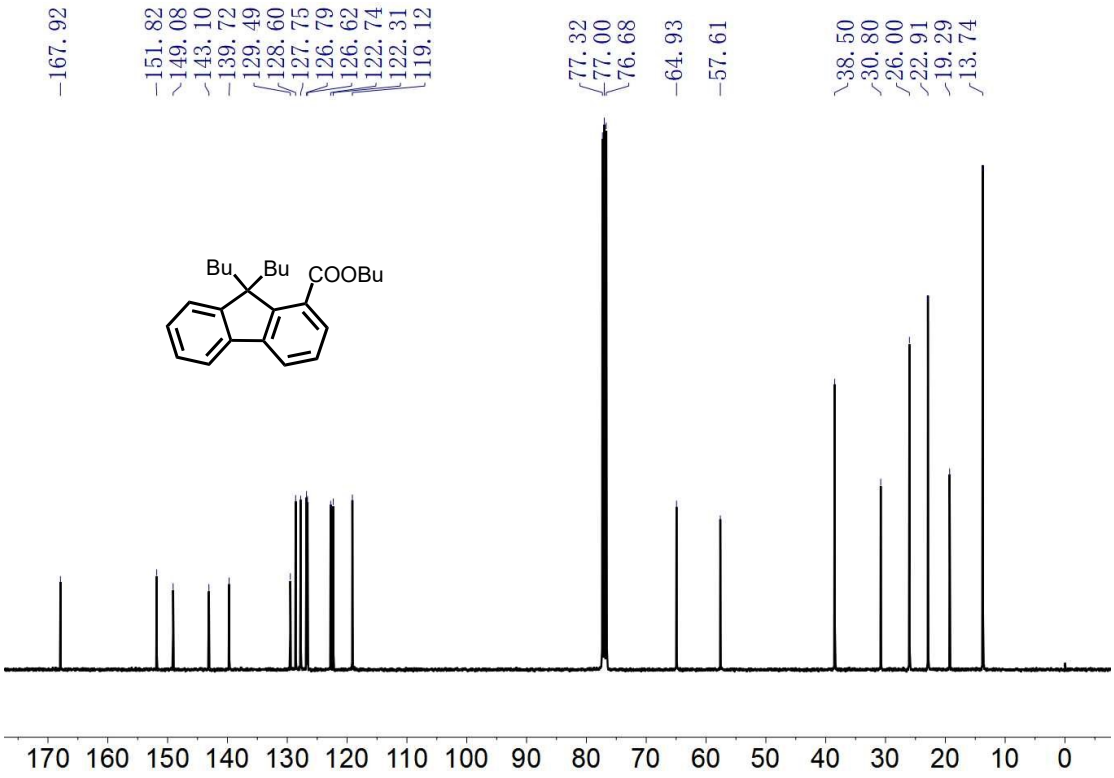

Figure S2. ^{13}C NMR spectrum for compound **1** ($CDCl_3$, 298K)

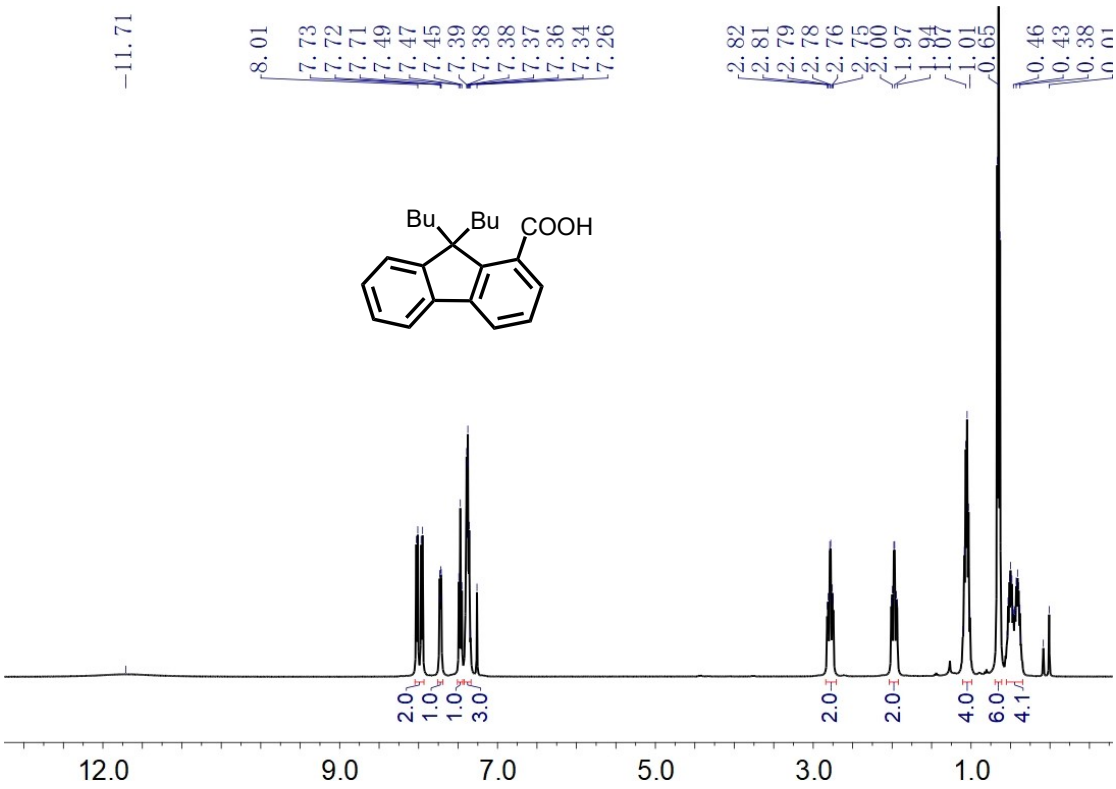

Figure S3. ^{1}H NMR spectrum for compound **2** ($CDCl_3$, 298K)

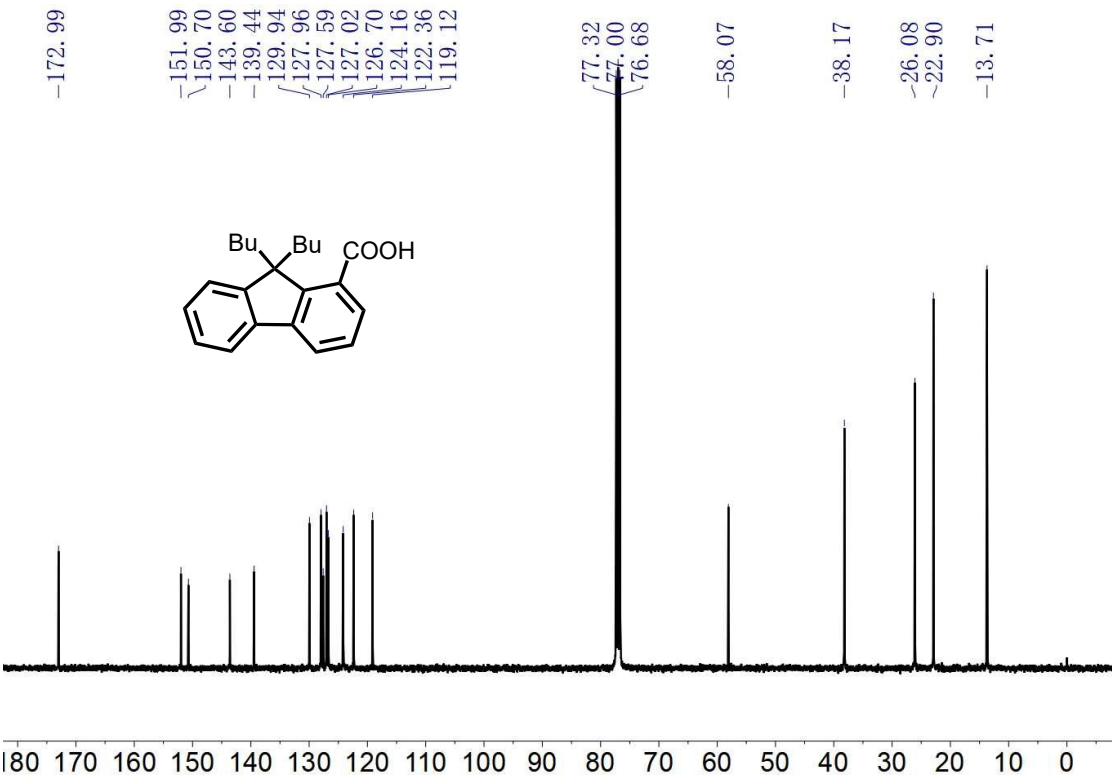

Figure S4. ^{13}C NMR spectrum for compound **2** ($CDCl_3$, 298K)

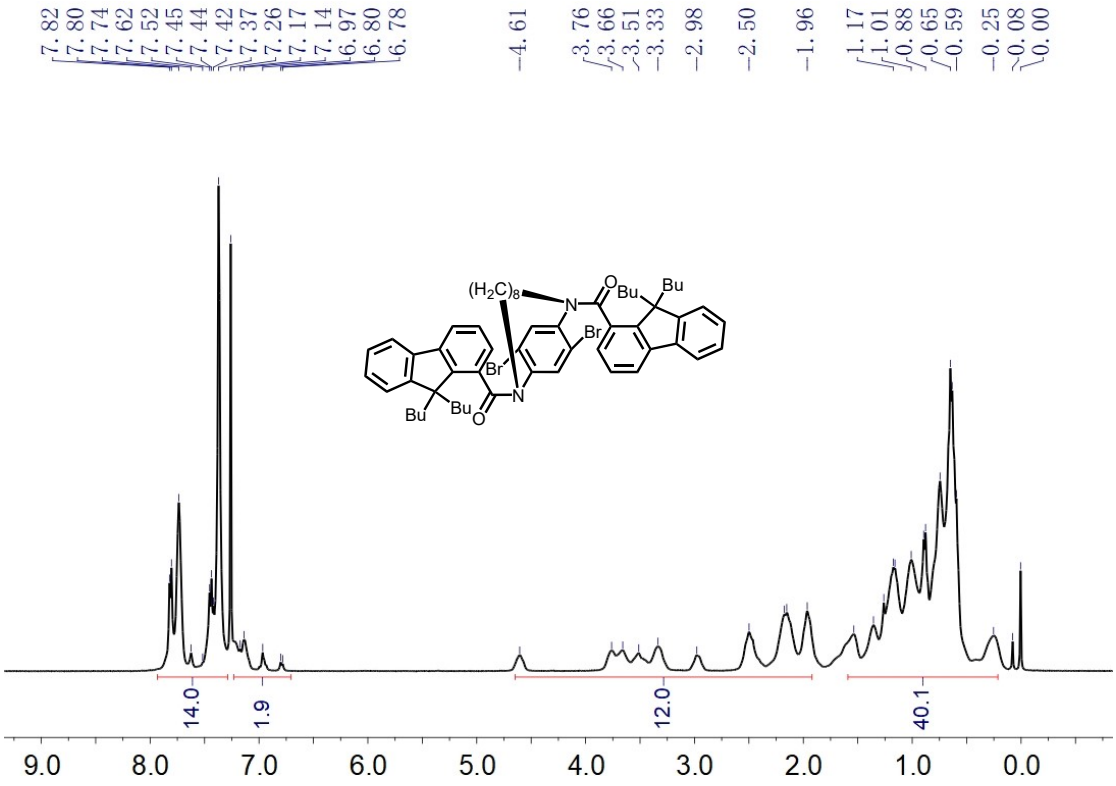

Figure S5. ^{1}H NMR spectrum for **(S_p)-2** ($CDCl_3$, 298K)

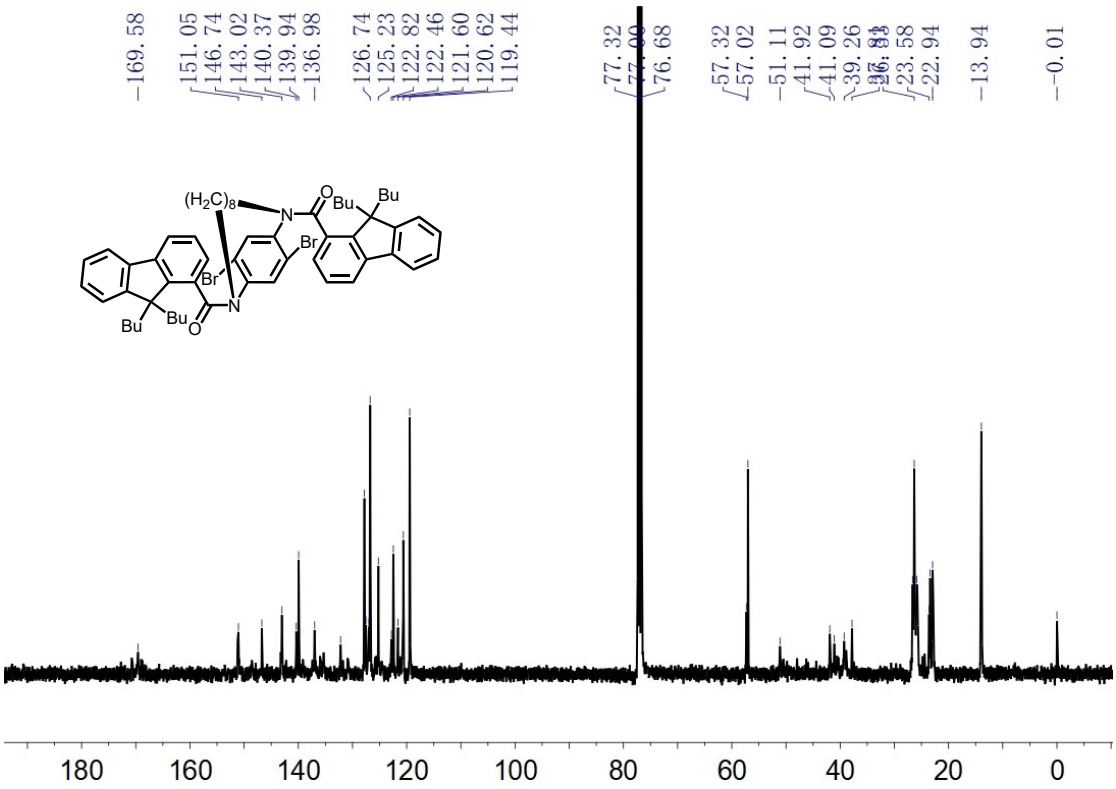

Figure S6. ^{13}C NMR spectrum for **(S_p)-2** ($CDCl_3$, 298K)

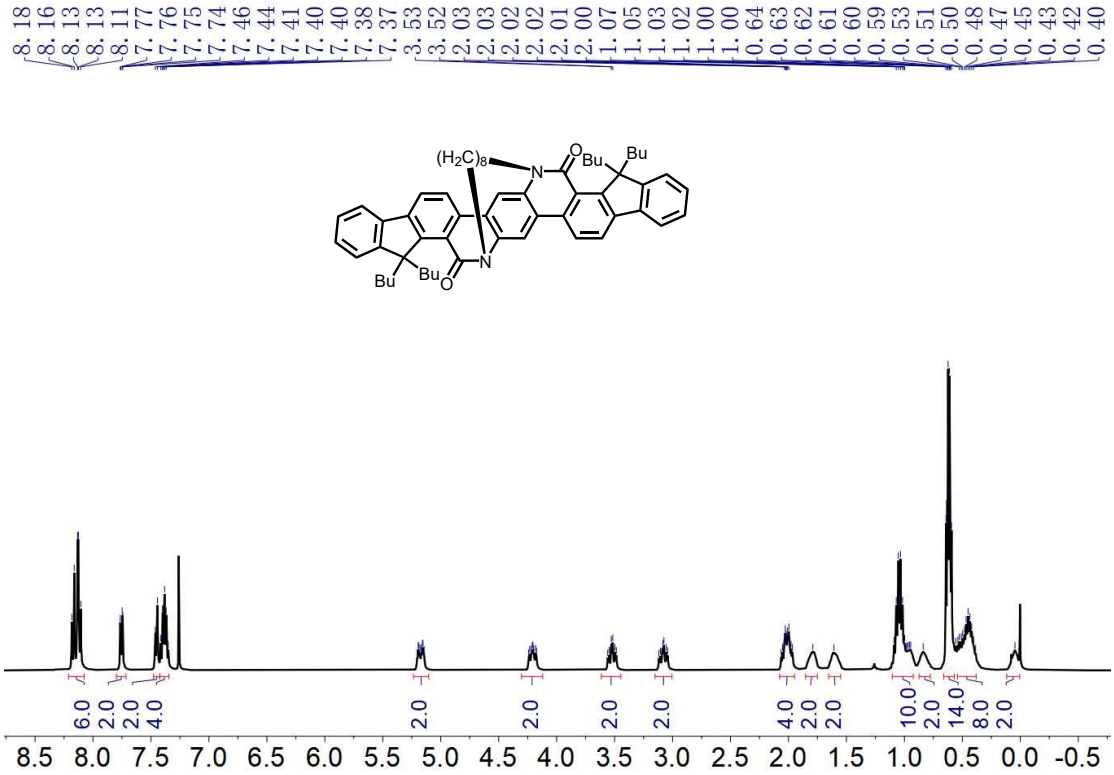

Figure S7. ^{1}H NMR spectrum for **(S_p)-3** ($CDCl_3$, 298K)

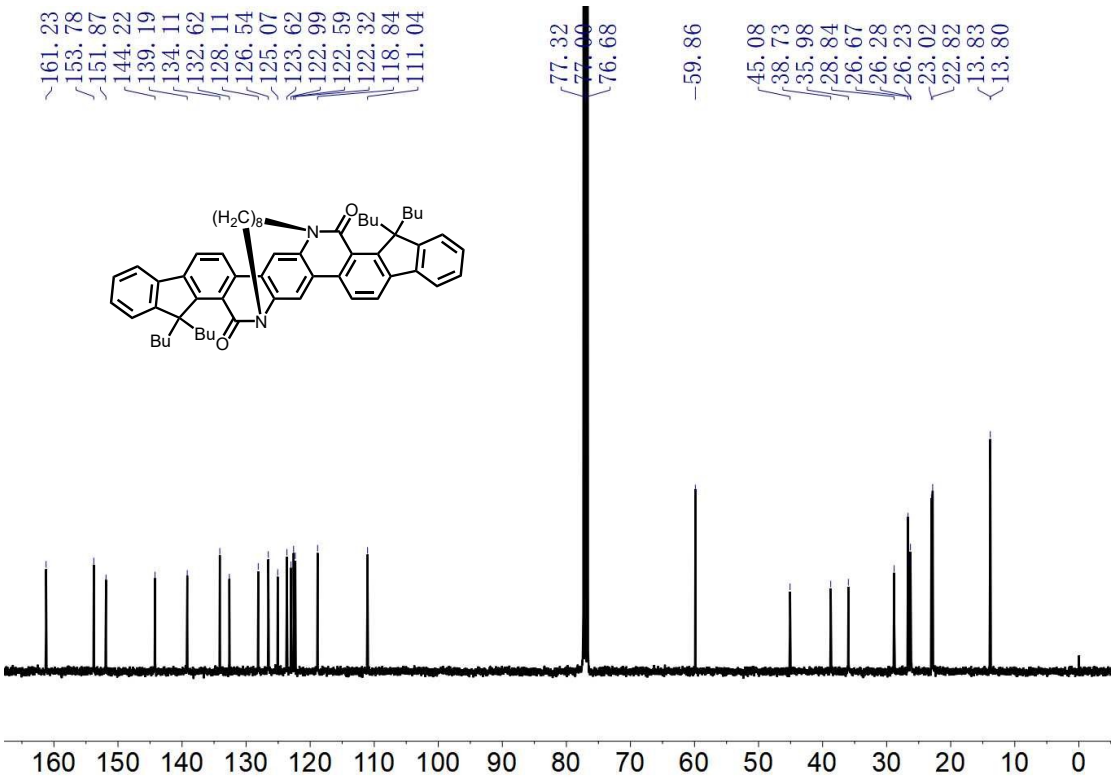

Figure S8. ^{13}C NMR spectrum for **(S_p)-3** ($CDCl_3$, 298K)

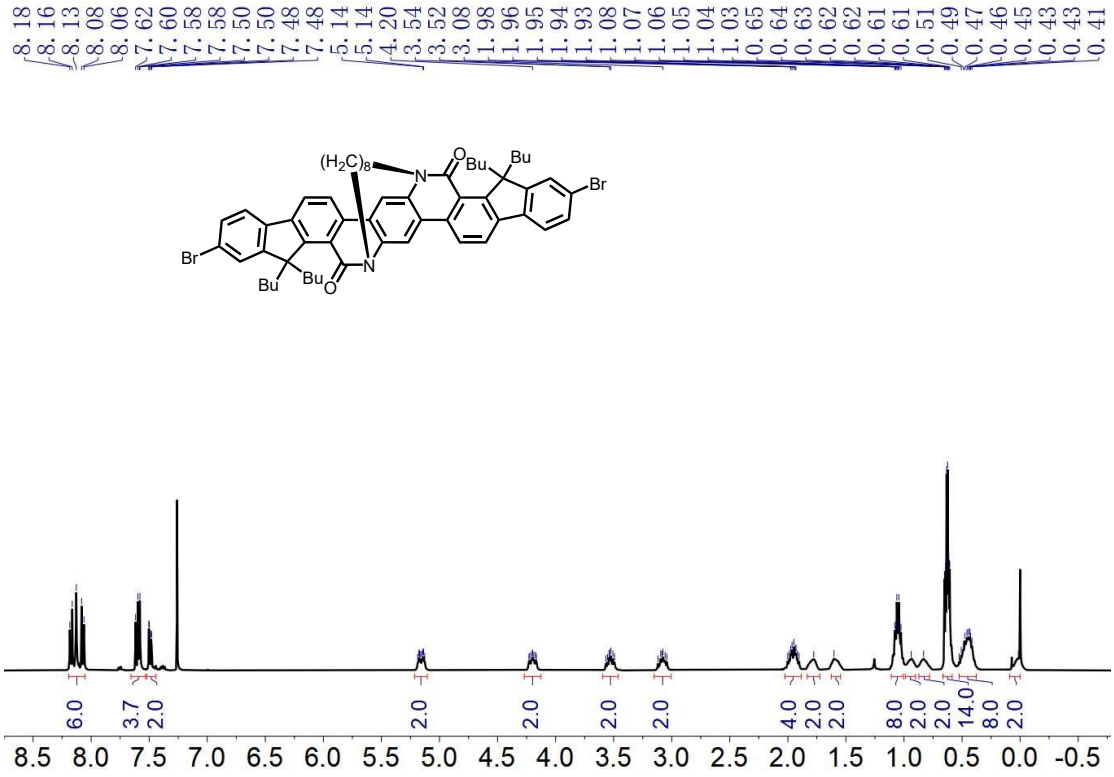

Figure S9. ^{1}H NMR spectrum for **(S_p)-4** ($CDCl_3$, 298K)

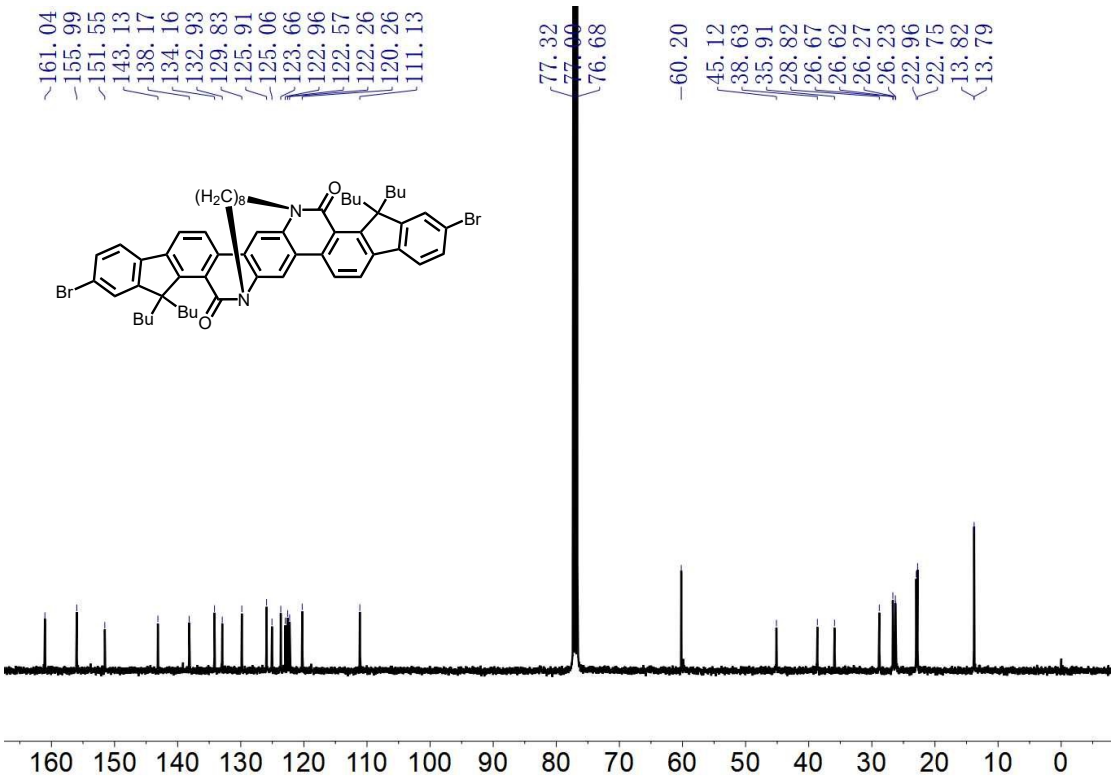

Figure S10. ^{13}C NMR spectrum for **(S_p)-4** ($CDCl_3$, 298K)

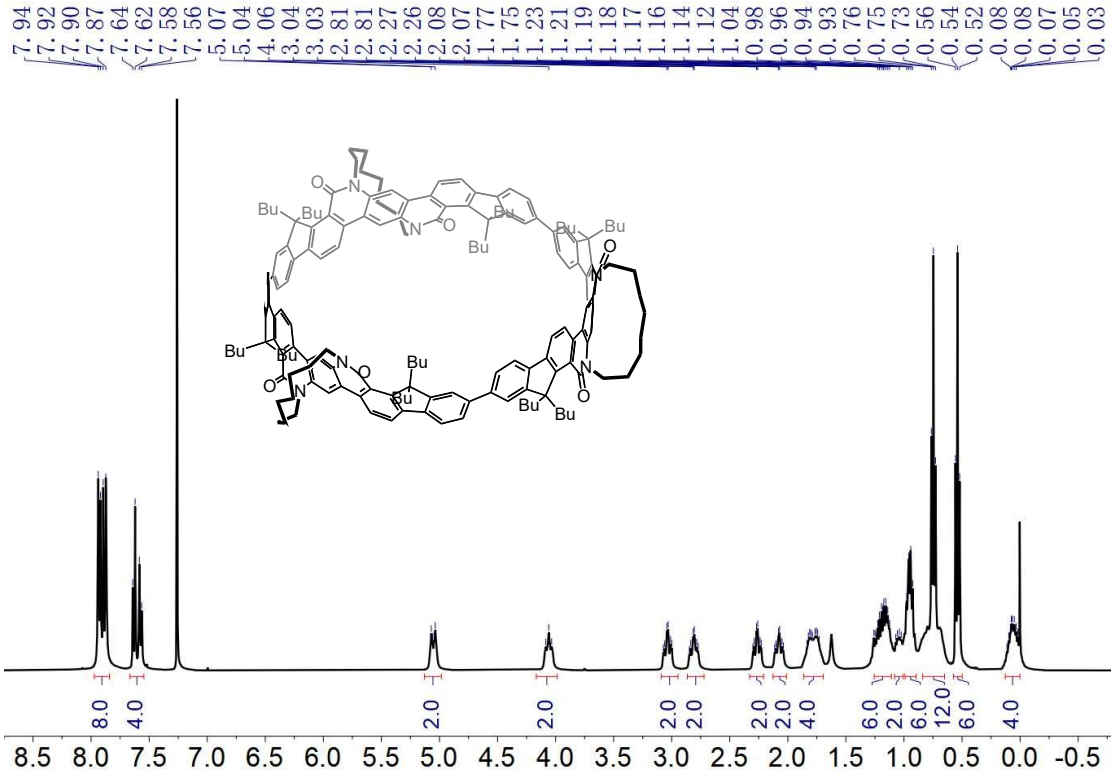

Figure S11. ^{1}H NMR spectrum for ***D*$_3$-(*P*)-NR5** ($CDCl_3$, 298K)

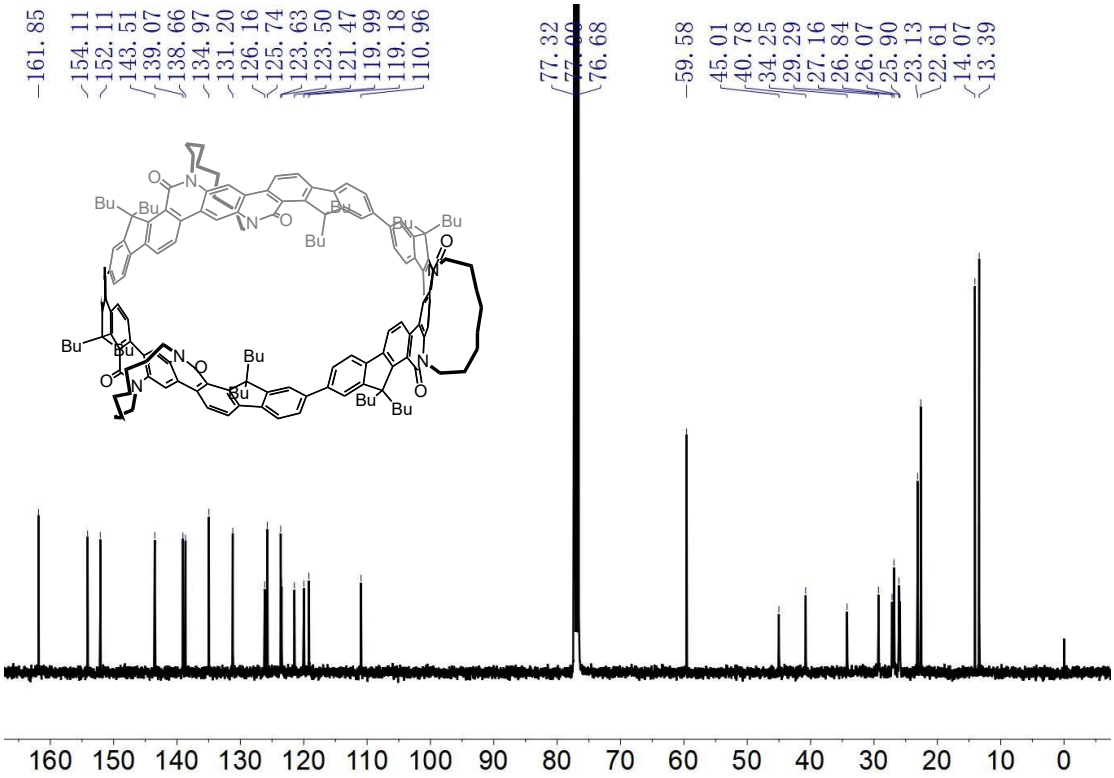

Figure S12. ^{13}C NMR spectrum for ***D*$_3$-(*P*)-NR5** ($CDCl_3$, 298K)

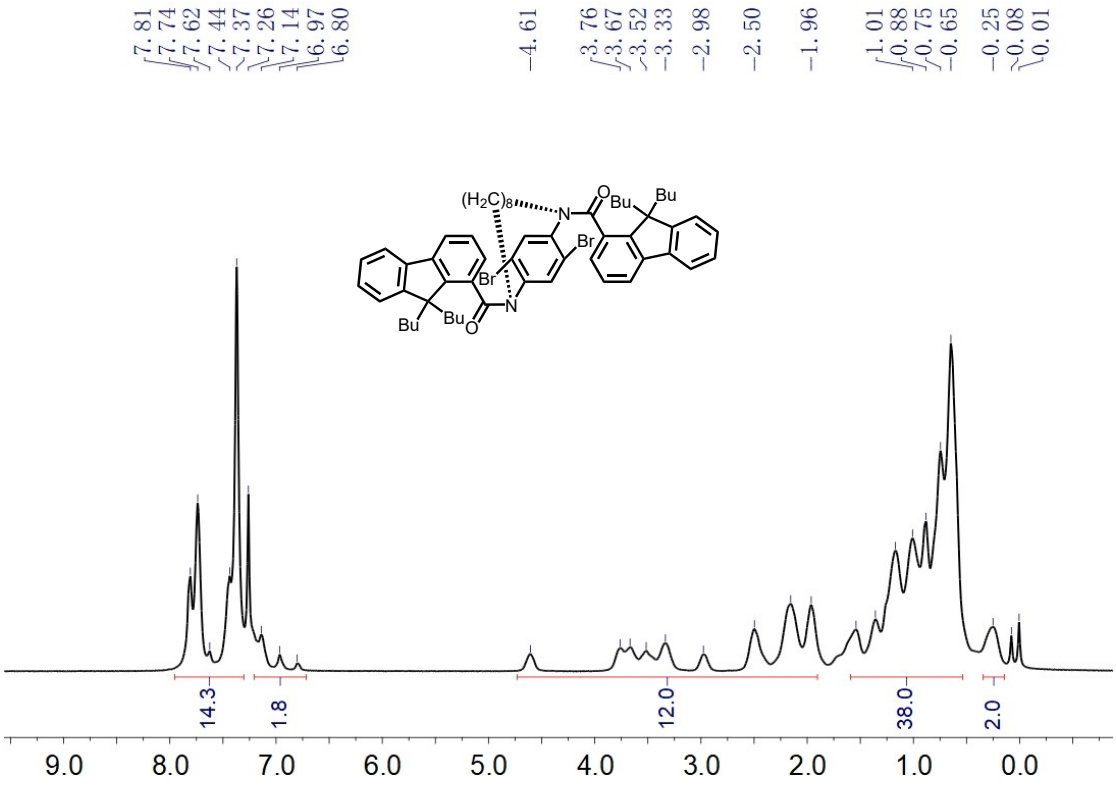

Figure S13. ^{1}H NMR spectrum for **(R_p)-2** ($CDCl_3$, 298K)

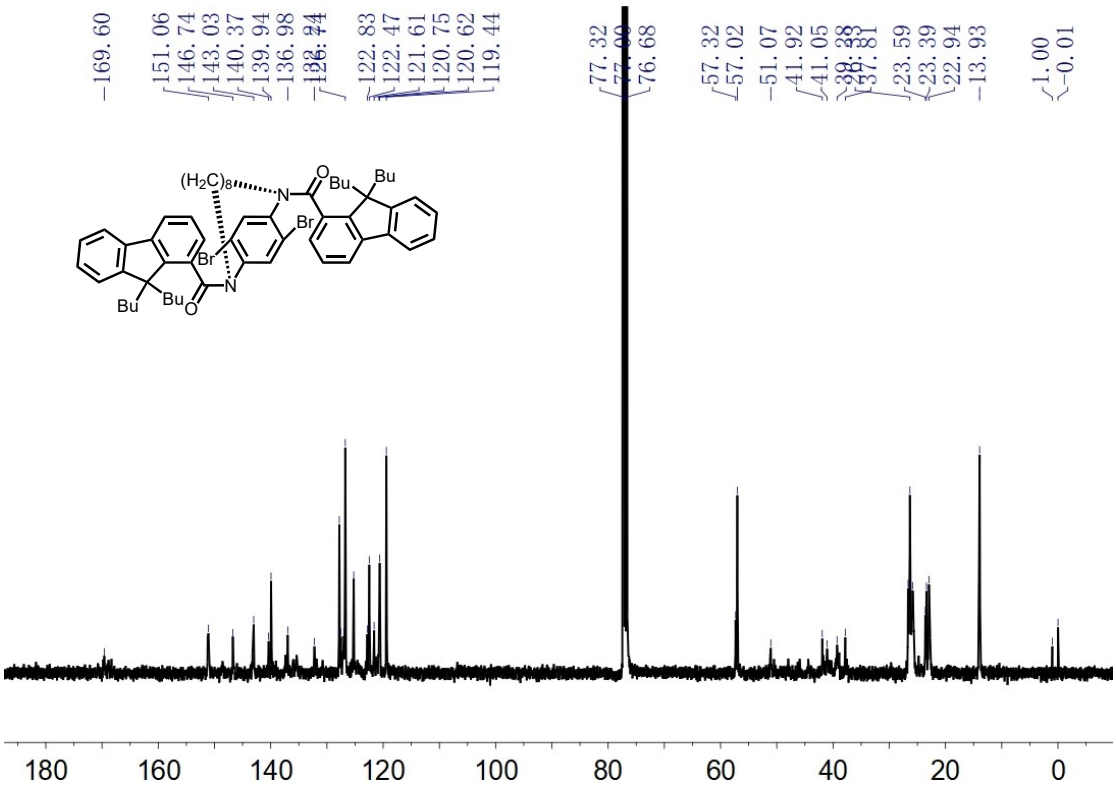

Figure S14. ^{13}C NMR spectrum for **(R_p)-2** ($CDCl_3$, 298K)

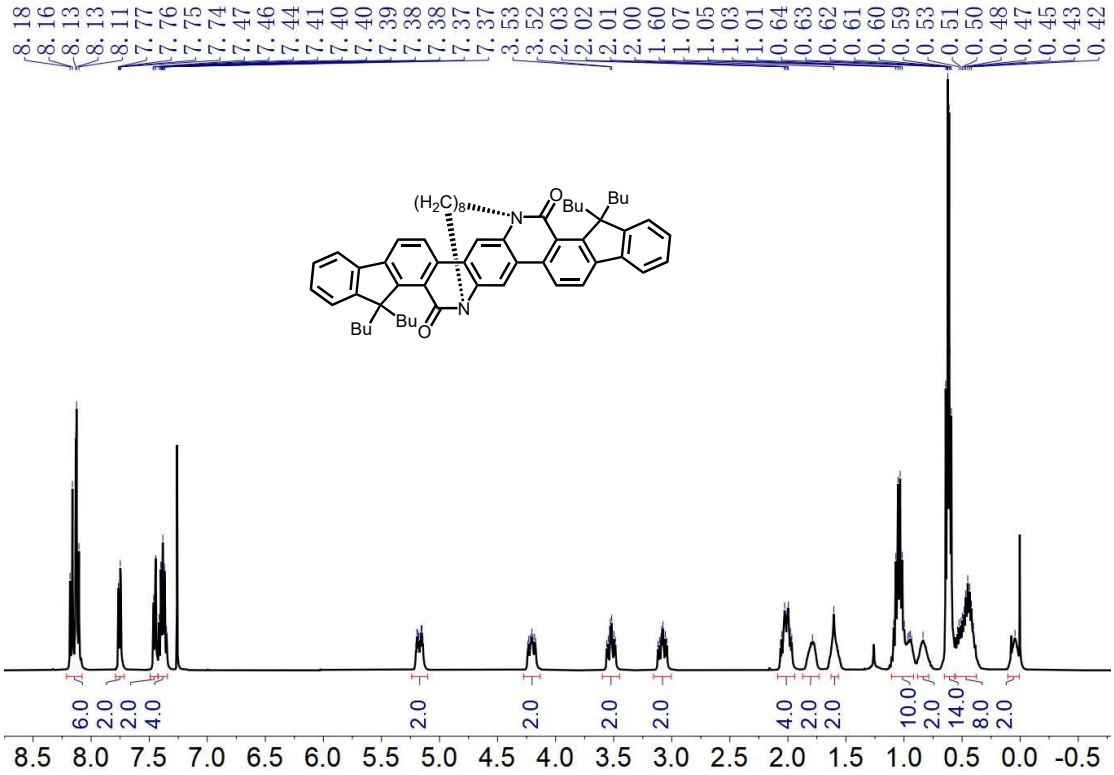

Figure S15. ^{1}H NMR spectrum for **(R_p)-3** ($CDCl_3$, 298K)

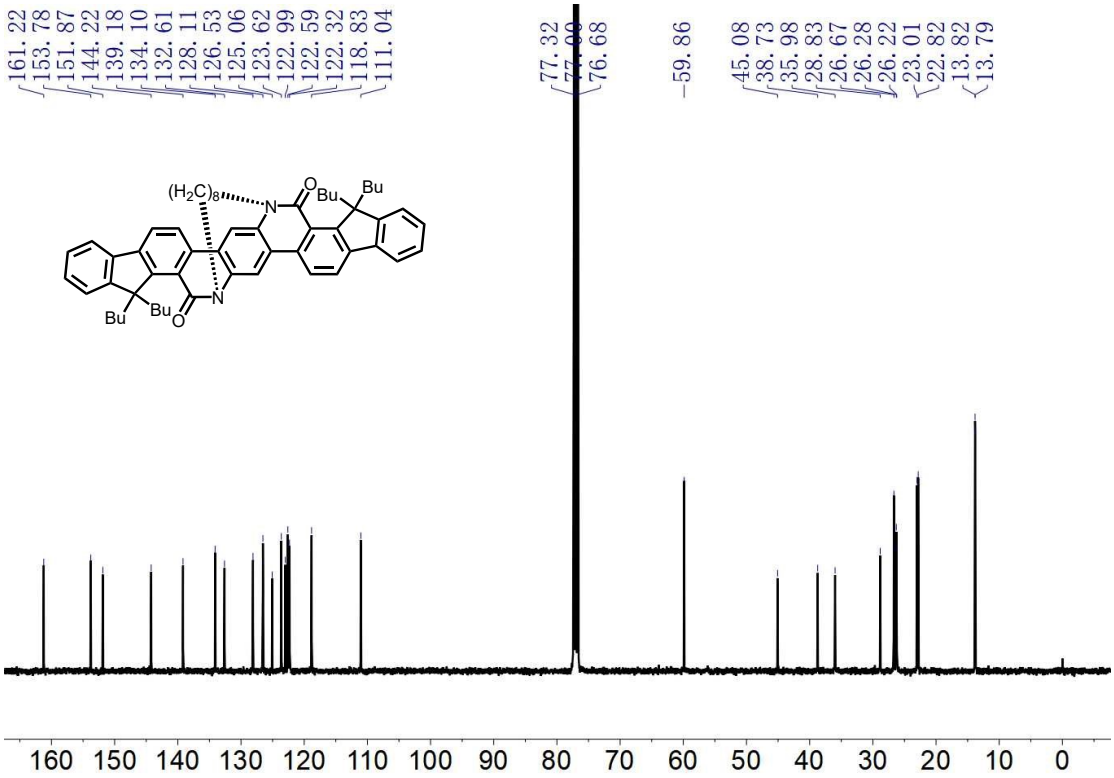

Figure S16. ^{13}C NMR spectrum for **(R_p)-3** ($CDCl_3$, 298K)

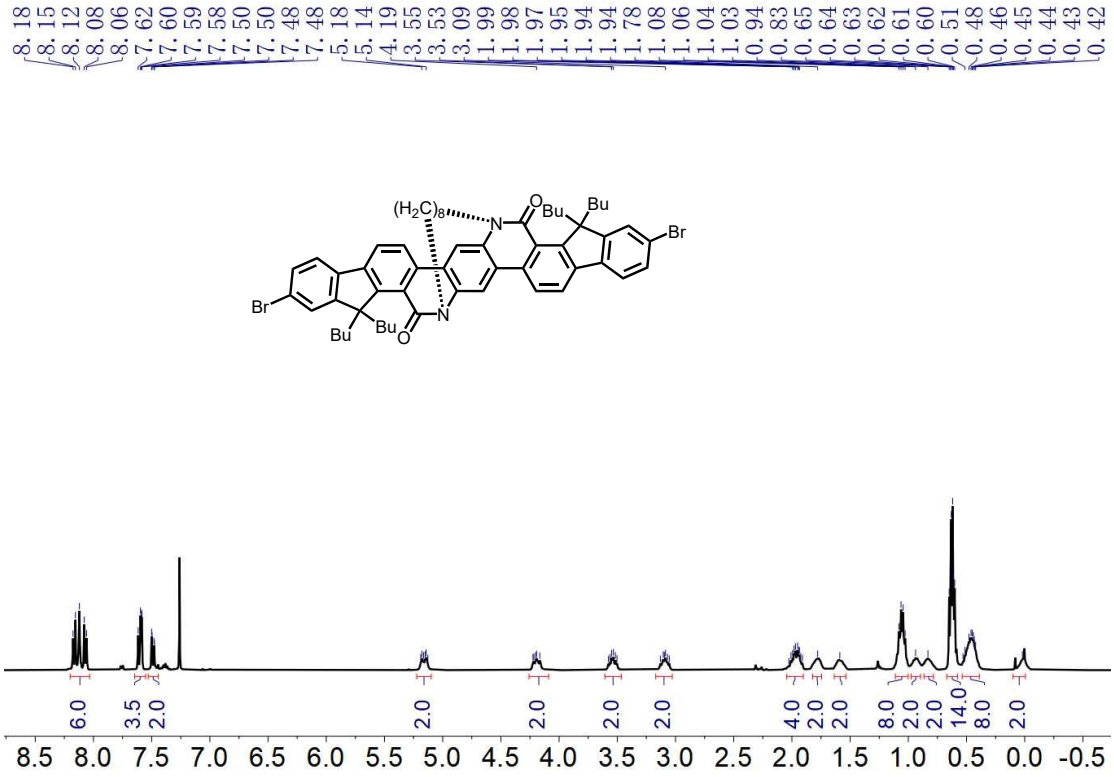

Figure S17. ^{1}H NMR spectrum for **(R_p)-4** ($CDCl_3$, 298K)

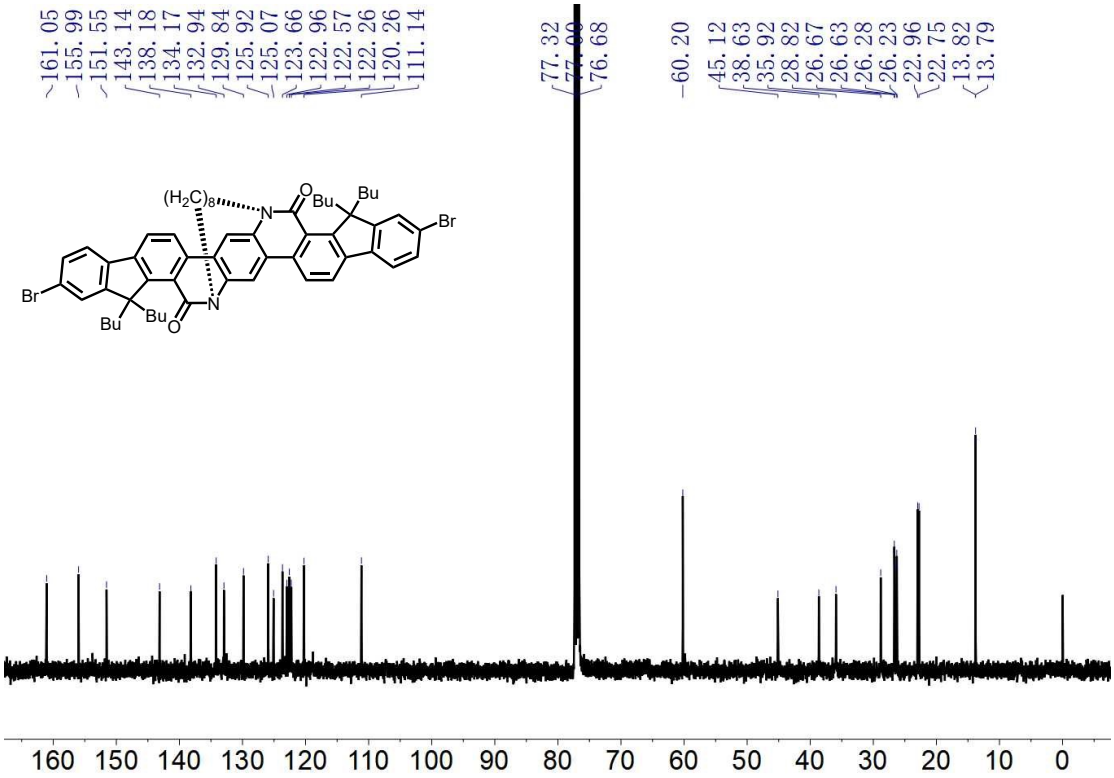

Figure S18. ^{13}C NMR spectrum for **(R_p)-4** ($CDCl_3$, 298K)

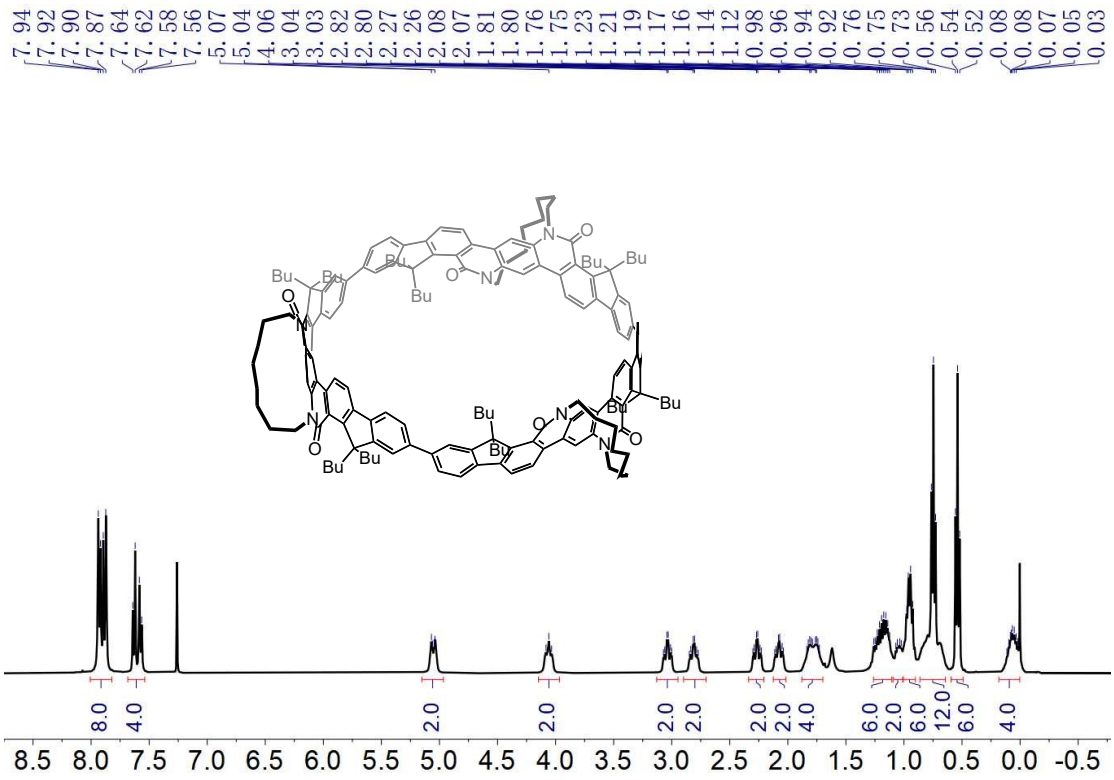

Figure S19. ^{1}H NMR spectrum for ***D*$_3$-(*M*)-NR5** ($CDCl_3$, 298K)

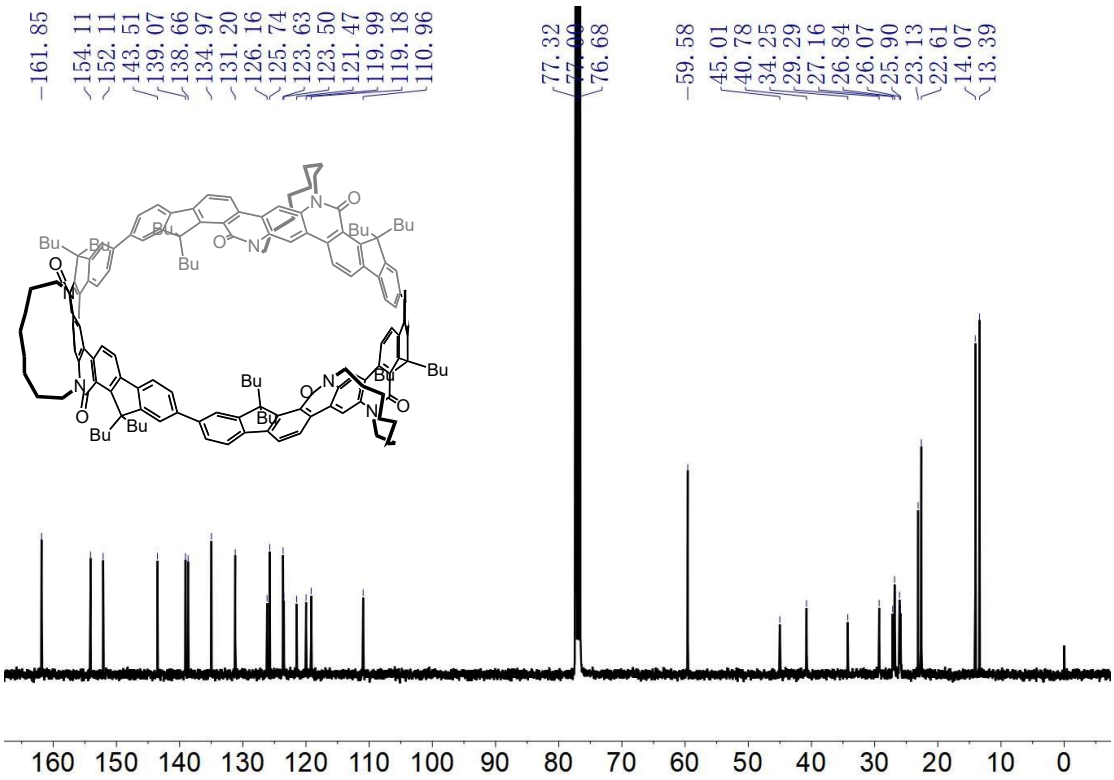

Figure S20. ^{13}C NMR spectrum for ***D*$_3$-(*M*)-NR5** ($CDCl_3$, 298K)

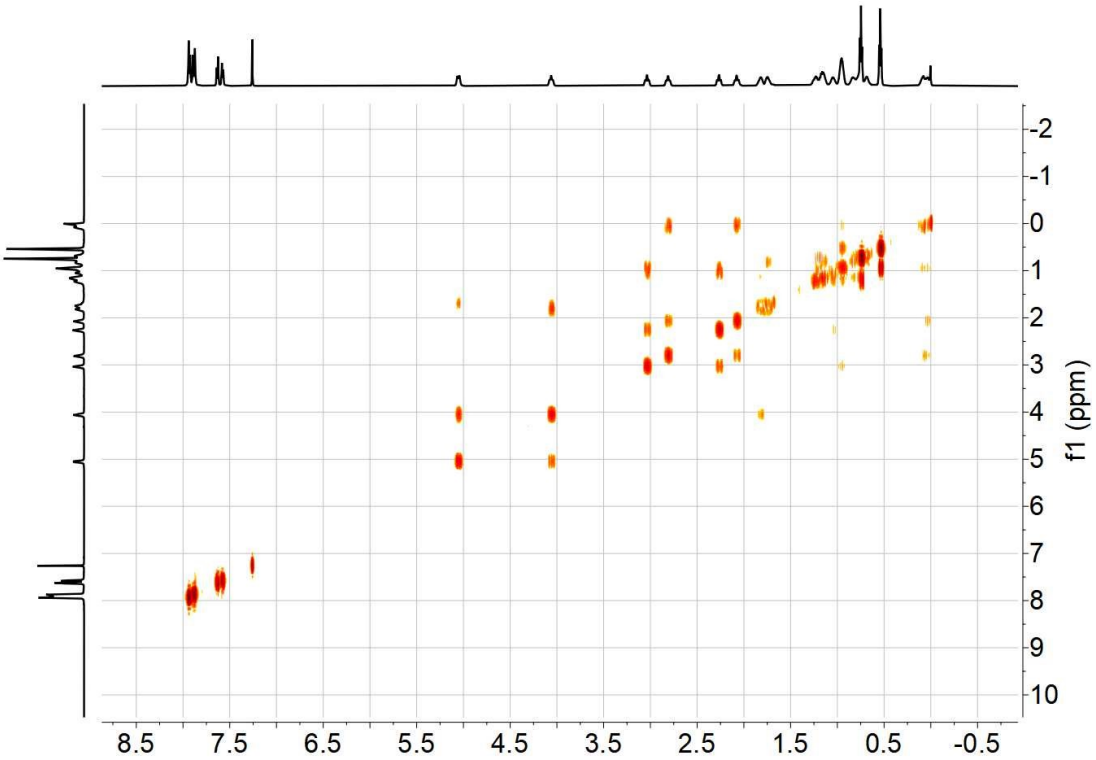

Figure S21. COSY spectrum for ***D*$_3$-(*P*)-NR5** ($CDCl_3$, 298K)

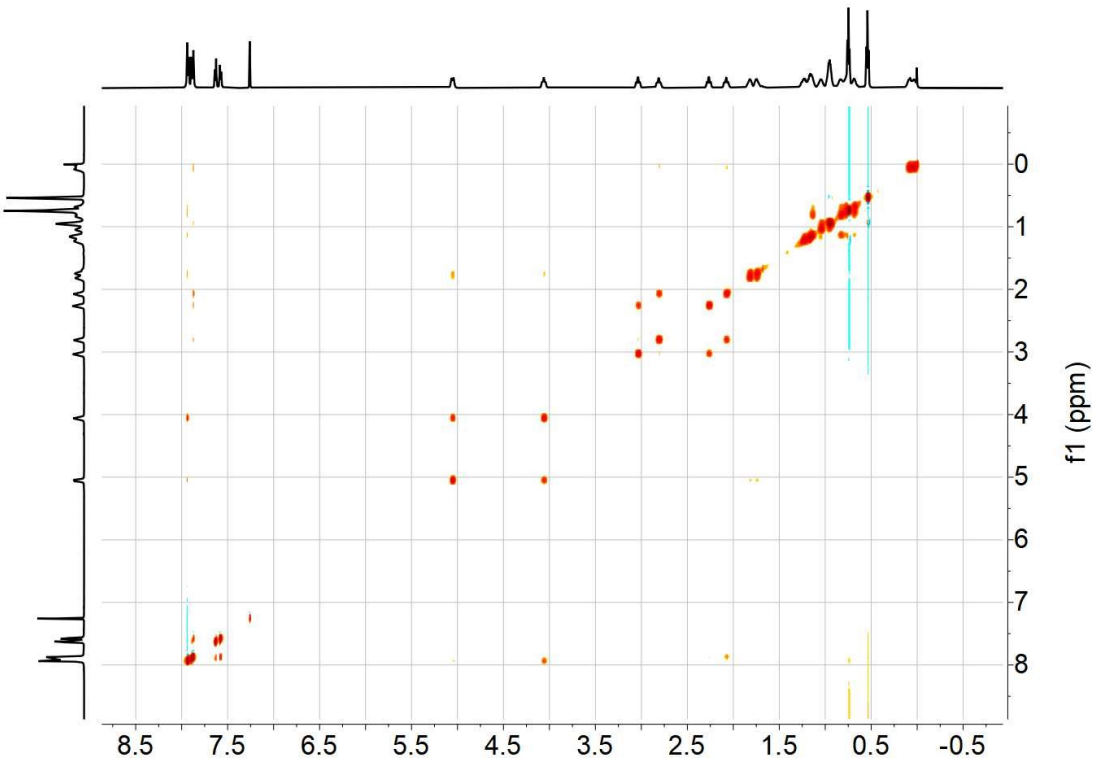

Figure S22. NOESY spectrum for ***D*$_3$-(*P*)-NR5** ($CDCl_3$, 298K)

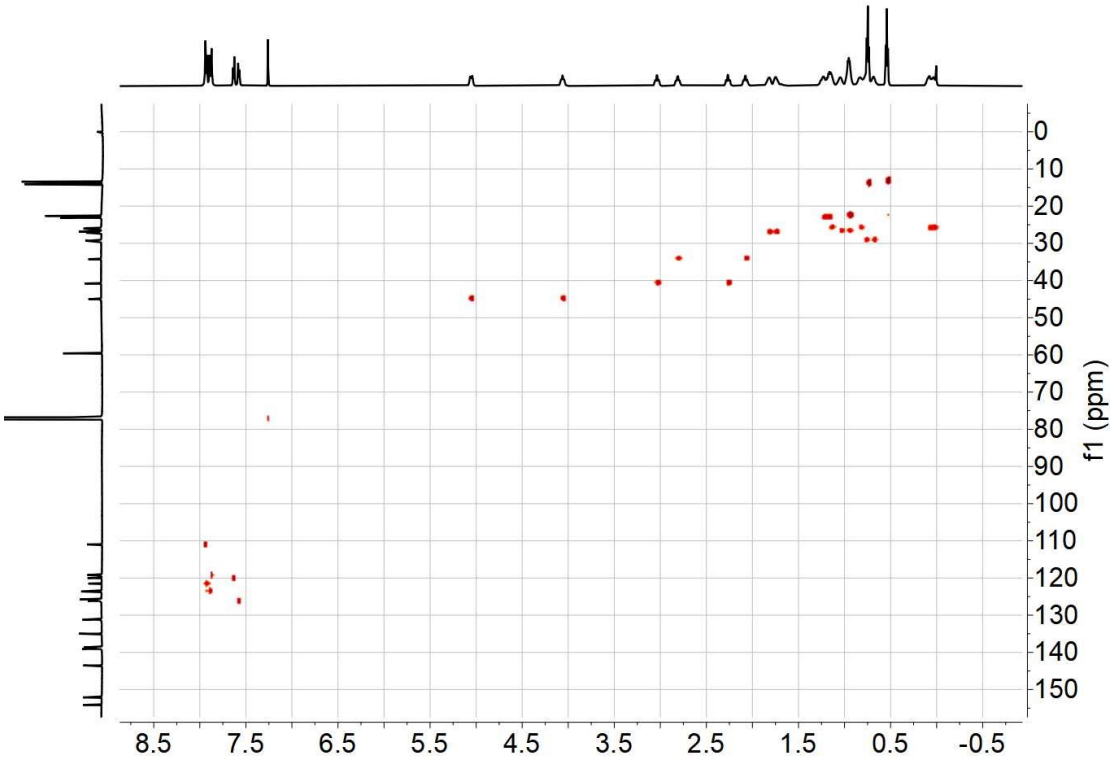

Figure S23. HSQC spectrum for ***D*$_3$-(*P*)-NR5** ($CDCl_3$, 298K)

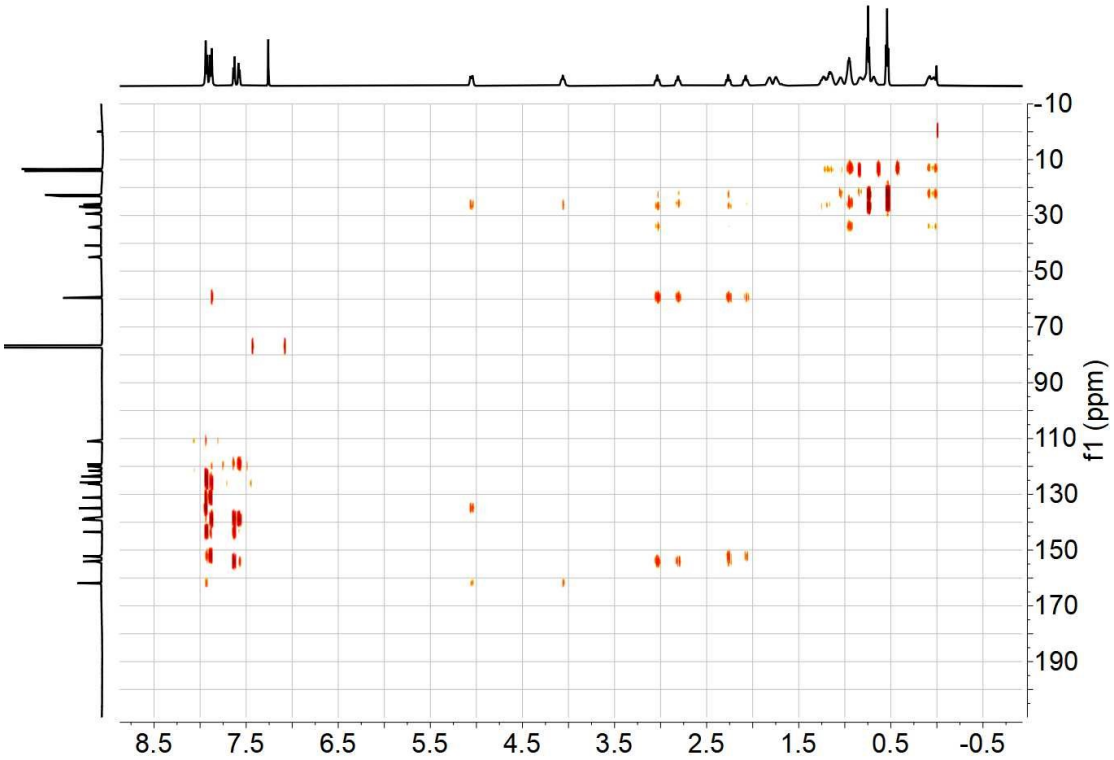

Figure S24. HMBC spectrum for ***D*$_3$-(*P*)-NR5** ($CDCl_3$, 298K)

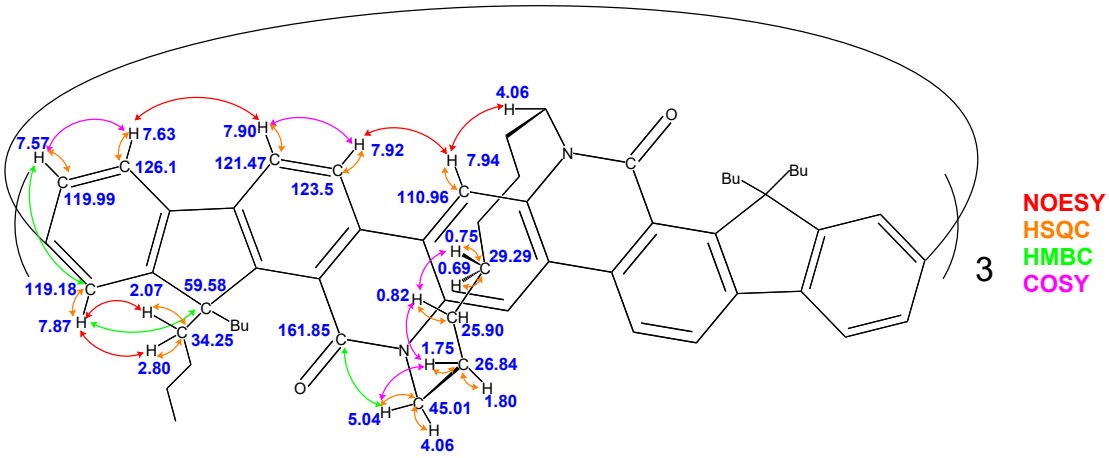

***D*$_3$-(*P*)-NR5**

Figure S25. A summary of the key correlations and assigned chemical shifts for ***D*$_3$-(*P*)-NR5**

5. IR spectra

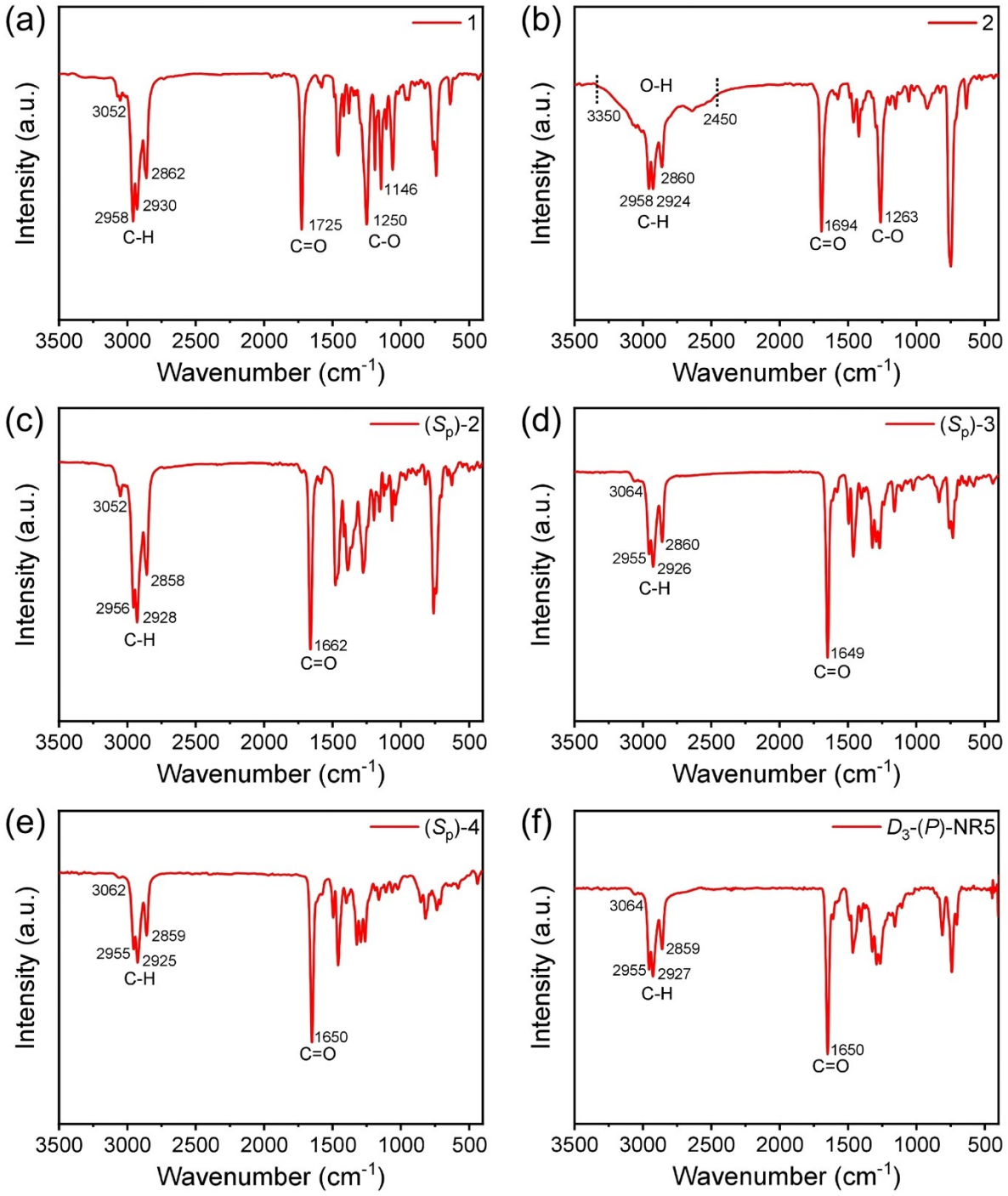

Figure S26. IR spectra of compound **1** (a), **2** (b), **(*S*$_p$)-2** (c), **(*S*$_p$)-3** (d), **(*S*$_p$)-4** (e) and ***D*$_3$-(*P*)-NR5** (f)

6. HRMS spectra

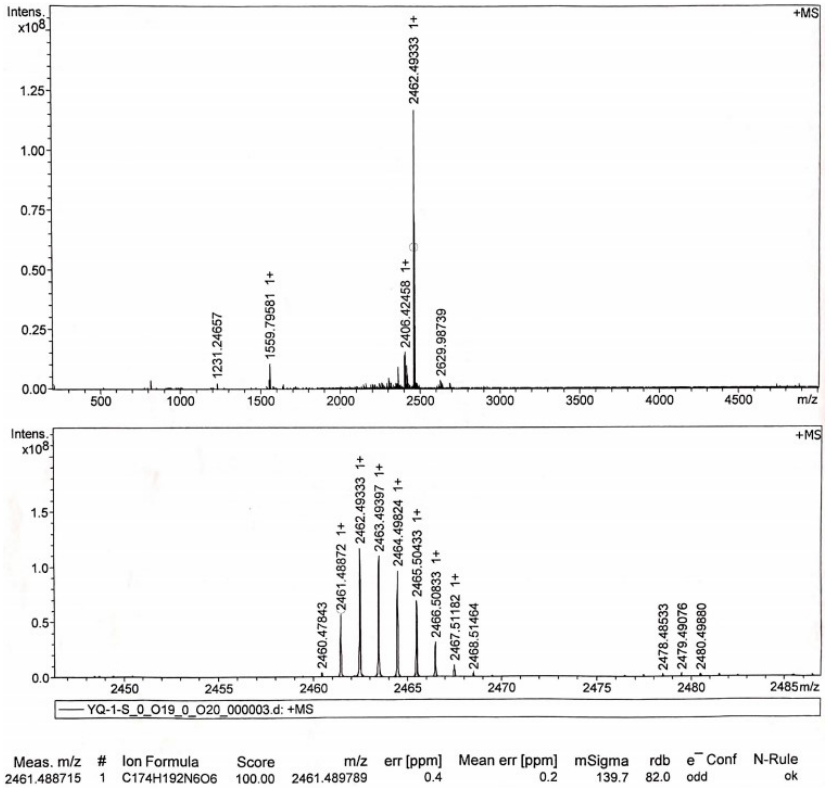

Meas. m/z	#	Ion Formula	Score	m/z	err [ppm]	Mean err [ppm]	mSigma	rdb	e⁻ Conf	N-Rule
2461.488715	1	C174H192N6O6	100.00	2461.489789	0.4	0.2	139.7	82.0	odd	ok

Figure S27. MALDI-TOF HRMS spectrum for ***D*$_3$-(*P*)-NR5**

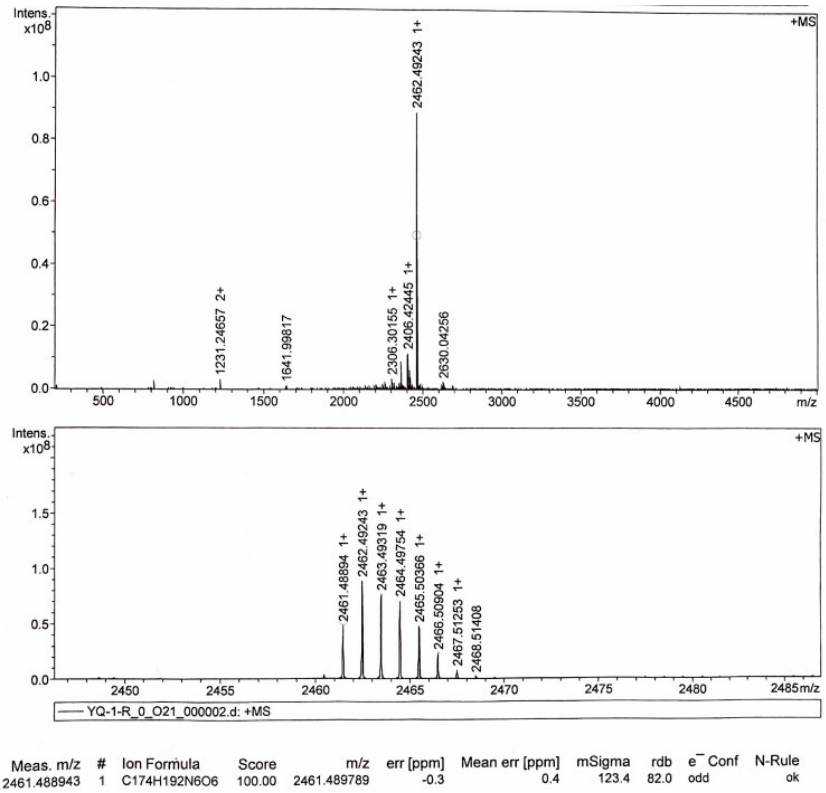

Meas. m/z	#	Ion Formula	Score	m/z	err [ppm]	Mean err [ppm]	mSigma	rdb	e⁻ Conf	N-Rule
2461.488943	1	C174H192N6O6	100.00	2461.489789	-0.3	0.4	123.4	82.0	odd	ok

Figure S28. MALDI-TOF HRMS spectrum for ***D*$_3$-(*M*)-NR5**

7. DFT calculation

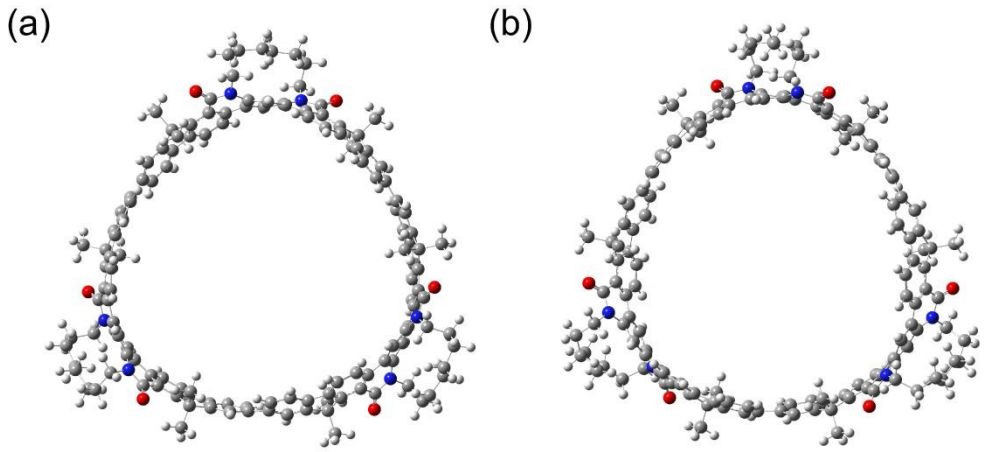

Figure S29. DFT-optimized ground state structures (a) and (b) for ***D*$_3$-(*P*)-NR5 and *D*$_3$-(*M*)-NR5**. Note: To reduce computation, replace butyl with methyl

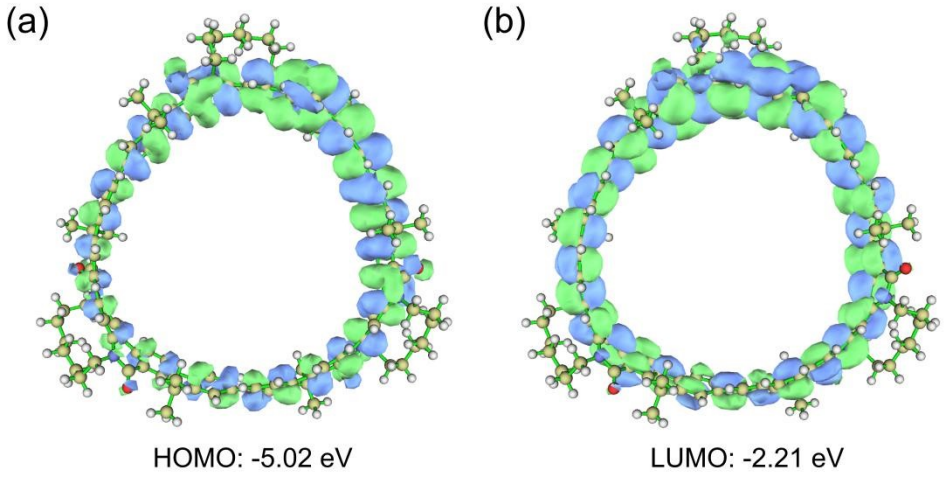

Figure S30. DFT-calculated HOMO (a) and LUMO (b) orbitals for ***D*$_3$-(*P*)-NR5**

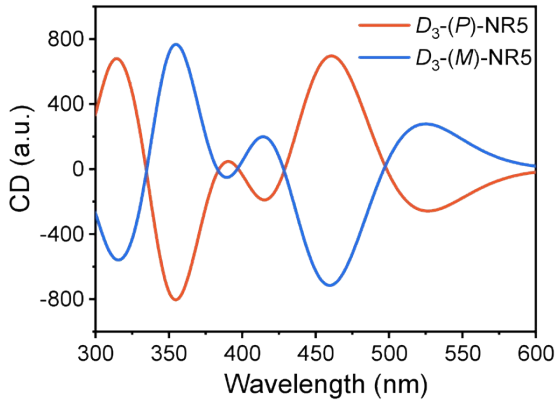

Figure S31. The theoretical CD spectra for ***D*$_3$-(*P*)-NR5 and *D*$_3$-(*M*)-NR5**

8. SHG performance

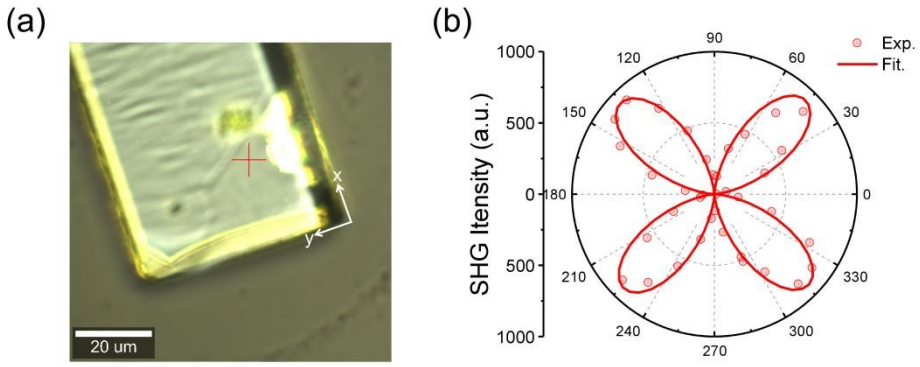

Figure S32. (a) Optical image of ***D*$_3$-(*P*)-NR5**. Note: The red + is where the pulse-laser is exciting. The x and y in the image correspond to 0° and 90° in polar SHG intensity plots. (b) The polarization dependence of SHG for D_3-(*P*)-NR5 crystals

The detected SHG intensity is proportional to the square of the induced second-order polarization (*P*) with the components $P_x(2\omega)$, $P_y(2\omega)$ and $P_z(2\omega)$. For crystal of D_3-(*P*)-NR5 (belonging to space group $P2_12_12$, point group 222), after considering the Kleinman's symmetry and intrinsic permutation symmetry, the specific relationship can be described by the following equation:[5]

$$\begin{bmatrix} P_x(2\omega) \\ P_y(2\omega) \\ P_z(2\omega) \end{bmatrix} = 2\varepsilon_0 \begin{bmatrix} 0 & 0 & 0 & d_{14} & 0 & 0 \\ 0 & 0 & 0 & 0 & d_{25} & 0 \\ 0 & 0 & 0 & 0 & 0 & d_{36} \end{bmatrix} \begin{bmatrix} E_x^2(\omega) \\ E_y^2(\omega) \\ E_z^2(\omega) \\ 2E_y(\omega)E_z(\omega) \\ 2E_x(\omega)E_z(\omega) \\ 2E_x(\omega)E_y(\omega) \end{bmatrix}$$

Where d_{ij} is the second-order susceptibility tensor of D_3-(*P*)-NR5 crystal, and $d_{14} = d_{25} = d_{36}$ according to the Kleinman's symmetry. E_x, E_y, and E_z represent the components of electric field. The detected SHG intensity (I_{SHG}) can be described by the function $I_{SHG}(\theta) \propto [2E^2 d_{14}\sin(2\theta)]^2$, where the angular parameter (θ) is defined as the azimuthal angle between the incident laser polarization and the D_3-(*P*)-NR5 crystal long axis. The above function can excellently fit the detected SHG intensity under different polarization angles (Figure S32b), further confirming the D_2 symmetry of the crystal.

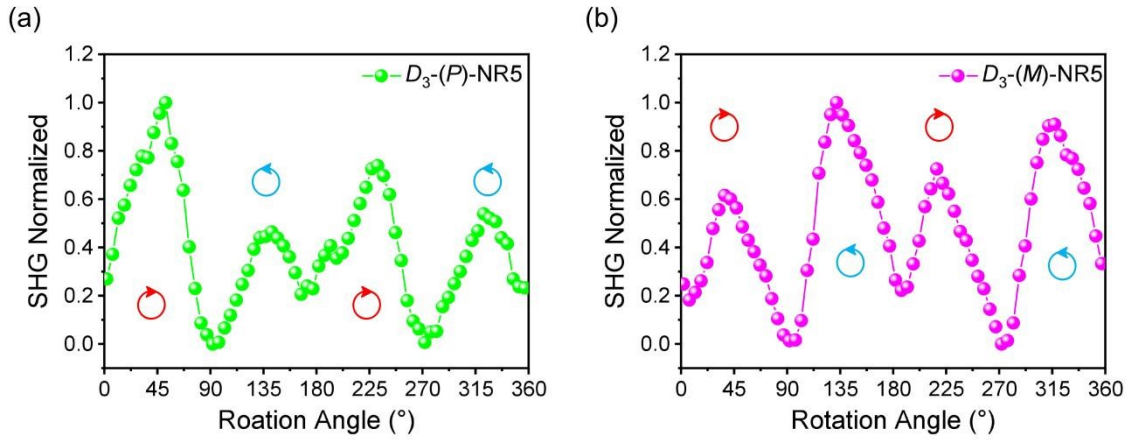

Figure S33. SHG intensity as a function of the rotation angle of the QWP for ***D*$_3$-(*P*)-NR5** (a) and ***D*$_3$-(*M*)-NR5** (b) single crystals

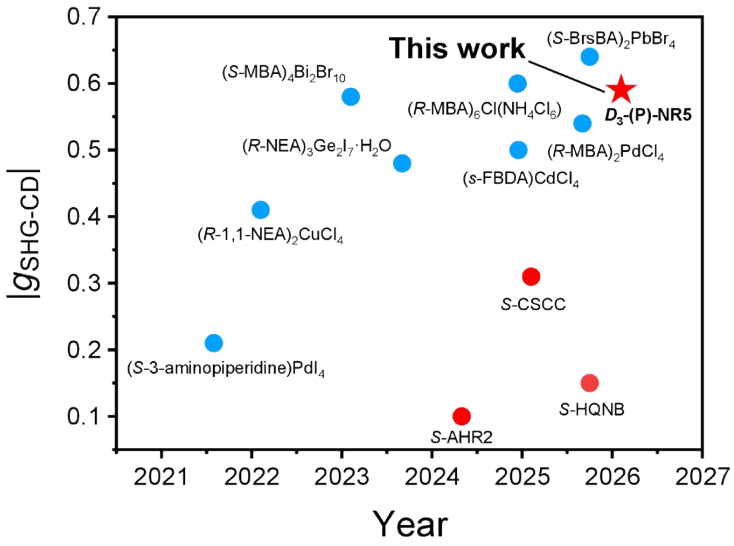

Figure S34. Comparison of $g_{SHG\text{-}CD}$ values in literature[6-16] with this work. Note: The red color represents purely organic materials and the blue color represents organic-inorganic hybrid materials. Circles represent compounds reported in the literature, and five-pointed stars represent compounds synthesized in this work

Table S1. Comparison of the $g_{SHG\text{-}CD}$ values with previously reported chiral organic and organic-inorganic hybrid materials

Chiral compounds	Category	$\lvert g_{SHG\text{-}CD}\rvert$	Ref.
D_3-(*P*)-NR5	organic material	0.59	this work
S-AHR2	organic material	0.10	6
S-CSCC	organic material	0.31	7
S-HQNB	organic material	0.15	8

(*S*-3-aminopiperidine)PdI_4	organic-inorganic hybrid materials	0.21	12
(*R*-1,1-NEA)$_2CuCl_4$	organic-inorganic hybrid materials	0.41	9
(*S*-MBA)$_4Bi_2Br_{10}$	organic-inorganic hybrid materials	0.58	13
(*R*-NEA)$_3Ge_2I_7 \cdot H_2O$	organic-inorganic hybrid materials	0.48	10
(*s*-FBDA)$CdCl_4$	organic-inorganic hybrid materials	0.50	14
(*R*-MBA)$_6Cl(NH_4Cl_6)$	organic-inorganic hybrid materials	0.6	16
(*R*-MBA)$_2PdCl_4$	organic-inorganic hybrid materials	0.54	15
(*S*-BrsBA)$_2PbBr_4$	organic-inorganic hybrid materials	0.64	11

Reference:

[1] G. M. Sheldrick, *Acta Cryst*., 2015, **A71**, 3−8.

[2] G. M. Sheldrick, *Acta Cryst.*, 2015, **C71**, 3−8.

[3] O. V. Dolomanov, L. J. Bourhis, R. J. Gildea, J. A. K. Howard and H. Puschmann, *J. Appl. Crystallogr.*, 2009, **42**, 339-341.

[4] Gaussian 16, Revision C.01, M. J. Frisch, G. W. Trucks, H. B. Schlegel, G. E. Scuseria, M. A. Robb, J. R. Cheeseman, G. Scalmani, V. Barone, G. A. Petersson, H. Nakatsuji, X. Li, M. Caricato, A. V. Marenich, J. Bloino, B. G. Janesko, R. Gomperts, B. Mennucci, H. P. Hratchian, J. V. Ortiz, A. F. Izmaylov, J. L. Sonnenberg, D. Williams-Young, F. Ding, F. Lipparini, F. Egidi, J. Goings, B. Peng, A. Petrone, T. Henderson, D. Ranasinghe, V. G. Zakrzewski, J. Gao, N. Rega, G. Zheng, W. Liang, M. Hada, M. Ehara, K. Toyota, R. Fukuda, J. Hasegawa, M. Ishida, T. Nakajima, Y. Honda, O. Kitao, H. Nakai, T. Vreven, K. Throssell, J. A. Montgomery, Jr., J. E. Peralta, F. Ogliaro, M. J. Bearpark, J. J. Heyd, E. N. Brothers, K. N. Kudin, V. N. Staroverov, T. A. Keith, R. Kobayashi, J. Normand, K. Raghavachari, A. P. Rendell, J. C. Burant, S. S. Iyengar, J. Tomasi, M. Cossi, J. M. Millam, M. Klene, C. Adamo, R. Cammi, J. W. Ochterski, R. L. Martin, K. Morokuma, O. Farkas, J. B. Foresman, and D. J. Fox, *Gaussian, Inc., Wallingford CT*, **2016**.

[5] D. A. Kleinman, *Phys. Rev.*, 1962, **126**, 1977-1979.

[6] L. Qin, J. Xie, B. Wu, H. Hong, S. Yang, Z. Ma, C. Li, G. Zhang, X.-S. Zhang, K. Liu and D. Zhang, *J. Am. Chem. Soc.*, 2024, **146**, 12206-12214.

[7] H. Peng, Y. Qin, X.-G. Chen, X.-J. Song, R.-G. Xiong and W.-Q. Liao, *Angew. Chem. Int. Ed.*, 2025, **64**, e202500285.

[8] Z.-Y. Yu, G.-F. Li, Z.-K. Xu, L. Long, Y. Qin, Z.-Y. Du and Z.-X. Wang, *Chin. J. Struct. Chem.*, 2025, **44**, 100715.

[9] Z. Guo, J. Li, J. Liang, C. Wang, X. Zhu and T. He, *Nano Lett.*, 2022, **22**, 846-852.

[10] H. Wang, J. Li, H. Lu, S. Gull, T. Shao, Y. Zhang, T. He, Y. Chen, T. He and G. Long, *Angew. Chem. Int. Ed.*, 2023, **62**, e202309600.
[11] J. Yu, M. Li, Y. Lv, B. Liao, G. Tan, J. Zou, X. Liu, Y. Han and L. Li, *Adv. Funct. Mater.*, 2025, e08904
[12] D. Fu, J. Xin, Y. He, S. Wu, X. Zhang, X.-M. Zhang and J. Luo, *Angew. Chem. Int. Ed.*, 2021, **60**, 20021-20026.
[13] X. Fu, Z. Zeng, S. Jiao, X. Wang, J. Wang, Y. Jiang, W. Zheng, D. Zhang, Z. Tian, Q. Li and A. Pan, *Nano Lett.*, 2023, **23**, 606-613.
[14] W. He, C. Chen, S. Wu, W. P. D. Wong, Z. Wu, K. Chang, J. Wang, H. Gao and K. P. Loh, *J. Am. Chem. Soc.*, 2025, **147**, 811-820.
[15] X. Qiu, J. Li, J. Zhu, H. Jin, T. He and G. P. Wang, *Angew. Chem. Int. Ed.*, 2025, **64**, e202510868.
[16] Z. Wang, X. Qiu, H. Wang, W. Zhao, S. Gull, H. Lu, Z. Hao, B. Sun, X. Zeng, X. Liu, H.-L. Zhang, Y. Chen, T. He and G. Long, *Angew. Chem. Int. Ed.*, 2025, **64**, e202420249.